Aerosol and Air Quality Research, 11: 187–209, 2011

ISSN: 1680-8584 print / 2071-1409 online
doi: 10.4209/aaqr.2010.10.0082

An Overview of Unipolar Charger Developments for Nanoparticle Charging

Panich Intra[1*], Nakorn Tippayawong[2]

[1] *College of Integrated Science and Technology, Rajamangala University of Technology Lanna, Chiang Mai, 50300, Thailand*
[2] *Department of Mechanical Engineering, Faculty of Engineering, Chiang Mai University, Chiang Mai, 50200, Thailand*

ABSTRACT

Charging of nanoparticles is an important process in aerosol sizing. A unipolar charger is one of the most important upstream components in aerosol particle sizing and measurement systems by electrical mobility analysis. The aim of particle charging for an electrical mobility analyzer is to impose a known net charge distribution on the aerosol particles for each size. Charger performance depends on the extrinsic charging efficiency and stable operation. A well-designed unipolar charger should provide high extrinsic charging efficiency and stability that can be accurately determined for any given operating conditions. Depending on the mechanisms used to generate the ionized gas, the chargers can be classified into: (i) a corona discharge chargers, (ii) a radioactive chargers, and (iii) a photoelectric chargers. In this article, a brief overview on the development of existing unipolar aerosol chargers for nanoparticles is presented. Descriptions of the operating principles as well as detailed physical characteristics of these chargers, including the corona discharge, ionizing radiation, and photoelectron emission, are given.

Keywords: Aerosol; Corona discharge; Ionizing radiation; Nanoparticles; Photoelectron emission; Unipolar charging.

INTRODUCTION

Nanoparticles possess many special physical, chemical and biological properties. They have found application in diverse fields, including materials synthesis, biotechnology, semiconductor manufacturing, pharmaceutical products, nano-composites and ceramics, emission control, health effects, instrumentation, and studies of fundamental transfer processes (Hinds, 1999). Nanoparticles are generally referred to as particles having a diameter in nanometer size range. Measurement capabilities are required to gain understanding of these particle dynamics. One of the most important steps in aerosol size measurement based on electrical mobility analysis is the particle charging mechanism. The purpose of the particle charging mechanism is to impose a known net charge distribution on the aerosol particles. Since particle size distribution is commonly determined through the electrical mobility classification, prediction of particle size requires the knowledge of the charge distribution for every particle size. High charging efficiency of aerosol particles results in high sensitivity of measurement. There are many mechanisms by which aerosol particles acquire net charge distributions. These are flame charging, static electrification, diffusion charging and field charging (Hinds, 1999). The most commonly used mechanism for charging particles in electrical measurement instruments is diffusion charging. Generally speaking, particles are allowed to collide with ions and the charge carried by these ions is transferred to the particles. This mechanism is so called due to the mechanism whereby ions travel in the gas and collide with the particles. There are three conventional ways to produce ions for diffusion charging in a gas; (i) by corona discharge, (ii) by photoelectric/UV-light sources, and (iii) by ionizing radiation from α-ray or β-ray sources such as ^{85}Kr, ^{241}Am, and ^{210}Po. Diffusion charging of particles can be unipolar or bipolar, depending on the polarity of the ions colliding to the particles.

Charging efficiency, defined as the fraction of charged particles among all the particles present at the charger downstream, is the most important performance parameter of an aerosol charger. For the bipolar diffusion charging, charging leads to a charge equilibrium which has low charging efficiencies, e.g., 3.3% and 5.7% for positively and negatively charged of 10 nm particles, respectively (Wiedensohler, 1988). In other words, over 90% of 10 nm particles would be neutral and could not be efficiently manipulated using electrostatic means. Unipolar diffusion charging has advantages over bipolar diffusion charging as it does not reach an equilibrium charge distribution, thereby potentially enabling the attainment of a higher

* Corresponding author. Tel.: +66-5392-1444;
Fax: +66-5321-3183
E-mail address: panich_intra@yahoo.com

charging efficiency. Additionally, particles can grow by Brownian coagulation in the bipolar diffusion charging if the aerosol particle number concentration is above about 10^7/cm^3 (Alonso and Alguacil, 2008). In general, the ideal charger would need a high efficiency charging technique with: (a) a stable and high ion concentration, (b) no damage to the aerosol, (c) low particle losses, (d) no contamination, (e) applicability to nanoparticles, and (f) capability of working at low pressures and in different gases.

The purpose of the present article is to give an overview of the state-of-the-art unipolar chargers for nanoparticles. Some of these chargers are commercially available and others are still laboratory prototypes. A detailed description of the operating principles as well as detailed physical characteristics of these chargers, including the corona discharge, ionizing radiation, and photoelectron emission, are presented.

UNIPOLAR DIFFUSION CHARGING THEORY

When an aerosol particle is exposed to gaseous ions, capture of ions by the particle occurs and leads to the appearance of an electrical charge on the particle. The magnitude of the charge depends upon the size of the particle, the unipolar ion density encountered, and the time that particle spends within this region. In the absence of any appreciable electric field, this particle will be diffusionally charged by the Brownian random motion of the ions with respect to the particle. In diffusion charging, the collisions between aerosol particles and ions are considered to occur in three regimes depending upon the magnitude of the Knudsen number, $Kn = \lambda_i/a$, where a is the particle radius and λ_i is the mean free path of ions. When the Knudsen number is small, i.e. $Kn \ll 1$, the process is diffusion controlled. Combination coefficients can then be obtained by solving the macroscopic diffusion equation. For large Knudsen numbers, i.e. $Kn \gg 1$, the kinetic theory of gases can be used to determine combination coefficients. However, in the intermediate Knudsen number range, i.e. $Kn \simeq 1$, the process is more complicated, and a number of approximate methods have been developed. The continuing work on ions and aerosols into the early 1950's produced many semi-empirical expressions for the rates of ion-aerosol attachment, under ion diffusion. This diffusion charging theory, which was among the first theories to give good agreement with experiments, was developed by Fuchs (1947), Bricard (1949) and Gunn (1955). Further theories were later developed by Bricard (1962) and Fuchs (1963), assuming that the ion diffuses to the particle and the diffusion equation is solved close to the particle. In Fuchs' theory, the boundary conditions used are that the fluxes due to diffusion and kinetic theory are equal at the limiting sphere, and that the ion density far from the particle, $n(\infty)$ is equal to the bulk ion concentration. This theory includes electrical image forces. Adachi *et al*. (1985) found good agreement between their experimental results and Fuchs' limiting sphere theory for particles in the transition regime ($Kn \simeq 1$) where the particle size is of similar magnitude to the ion mean free path. A common approach for solving the diffusion charging problem in unipolar ionized gases is based on the birth-and-death theory proposed by Boisdron and Brock (1970). The evolution of the charge distribution on monodisperse particles is given by the solution of an infinite set of differential-difference equations (DDEs) as follows in Eqs. (1) to (3) (Biskos, 2004)

$$\frac{\mathrm{d}N_{p,0}}{\mathrm{d}t} = -\beta N_{p,0} N_i \tag{1}$$

$$\frac{\mathrm{d}N_{p,1}}{\mathrm{d}t} = \beta_0 N_{p,0} N_i - \beta_1 N_{p,1} N_i \tag{2}$$

$$\frac{\mathrm{d}N_{p,n}}{\mathrm{d}t} = \beta_{n-1} N_{p,n-1} N_i - \beta_n N_{p,n} N_i \tag{3}$$

Here, $N_{p,n}$ is the number concentration of aerosol particles with n elementary charges, N_i is the ion concentration, and β_n is the combination coefficient of ions with particles carrying n elementary charges. The equation for combination coefficient (Adachi *et al*., 1985) based on the particle charging theory by Fuchs (1963) is shown by Eq. (4), where x, $\phi(r)$ and δ are defined by Eqs. (5) to (7), respectively.

$$\beta_n = \frac{J_n}{N_i} = \frac{\pi\gamma\bar{c}_i\delta^2 \exp\left(-\dfrac{\phi(\delta)}{kT}\right)}{1+\exp\left(-\dfrac{\phi(\delta)}{kT}\right)\dfrac{\pi\gamma\bar{c}_i\delta^2}{4D_i a}\displaystyle\int_0^{a/\delta}\exp\left(\frac{\phi(a/x)}{kT}\right)\mathrm{d}x} \tag{4}$$

$$x = a/r \tag{5}$$

$$\phi(r) = \int_r^\infty F(r)\mathrm{d}r = \frac{pe^2}{4\pi\varepsilon_0 r} - \frac{\varepsilon_1 - 1}{\varepsilon_1 + 1}\frac{e^2}{8\pi\varepsilon_0}\frac{a^3}{r^2(r^2-a^2)} \tag{6}$$

$$\delta = \frac{a^3}{\lambda_i^2}\left[\frac{\left(1+\dfrac{\lambda_i}{a}\right)^5}{5} - \frac{\left(1+\dfrac{\lambda_i^2}{a^2}\right)\left(1+\dfrac{\lambda_i}{a}\right)^3}{3} + \frac{2}{15}\left(1+\frac{\lambda_i^2}{a^2}\right)^{5/2}\right] \tag{7}$$

$\phi(r)$ is the electrostatic potential of the ions at distance r from the center of the particle, $F(r)$ is the force of electrostatic interaction between the ion and the p-charged particle, δ is the radius of the limiting-sphere, $J_n = \mathrm{d}n/\mathrm{d}t$ is the flux of ions to the particle, γ is the probability of an ion entering the limiting-sphere to collide and transfer its charge to the particle, $\bar{c}_i$ is the mean thermal speed of the ions, D_i is the diffusion coefficient of ions, λ_i is the mean free path of ions, k is the Boltzmann's constant (1.380658 $\times 10^{-23}$ J/K), T is the operating temperature of the system, a is the particle radius, e is the elementary electrical charge, ε_0 is the dielectric constant of vacuum, and ε_1 is the relative

permittivity of particle material. A simultaneous solution of the above system of DDEs provides the average charge and charge distribution on particles of a specific diameter exposed to given charging conditions ($N_i t$ product).

However, it is possible to consider the process of diffusion charging in a simpler way, and develop a crude theory to estimate particle charges. This was done by White (1951, 1963) who derived a free molecule theory by considering the flux of ions impinging on the particle surface and using the Boltzmann distribution for the spatial distribution of ions. It can be expressed in a convenient analytic form. For particles whose radii are slightly greater than their mean free path, ions diffusion and collision with aerosol particles are predicted by kinetic theory. The collision rate (and therefore the charging rate) is proportional to the thermal speeds of ions and the capture area of the aerosol particles. In White's theory, the ion is assumed to stick to the particle after each collision. For an initially neutral particle immersed in a unipolar ion cloud, the flux of ions, J, impinging on the particle surface area is given by Eq. (8).

$$J = 4\pi a^2 \left(\bar{c}_i \frac{N_s}{4} \right) \tag{8}$$

Here, N_s is the concentration of ions above the surface. The spatial distribution of ions is given by the classical Boltzmann distribution for the equilibrium state. Neglecting the image force attraction between the ions and the particle, the Boltzmann distribution at the particle surface is given by Eq. (9).

$$N_s = N_i \exp\left(-K_E \frac{n_p e^2}{akT} \right) \tag{9}$$

Here, n_p is the particle charge, and $K_E = 1/4\pi\varepsilon_0$ with the vacuum permittivity. Substituting Eq. (9) into Eq. (8) gives Eq. (10).

$$J = \pi a^2 \bar{c}_i N_i \exp\left(-K_E \frac{n_p e^2}{akT} \right) \tag{10}$$

The above equation was originally derived by White (1951, 1963). The charging rate expression can be described by a system of differential equation as shown by Eq. (11).

$$\frac{\mathrm{d}n_p}{\mathrm{d}t} = \pi a^2 \bar{c}_i N_i \exp\left(-K_E \frac{n_p e^2}{akT} \right) \tag{11}$$

The integrated form of the above equation is widely used and can be found in standard textbooks (Willeke and Baron, 1993; Hinds, 1999). With the initial condition that $n_p = 0$ at $t = 0$ for the charging of an aerosol (initially neutral), the average charge of a particle can be integrated analytically to give Eq. (12).

$$\int_0^{n_p} \frac{\mathrm{d}n_p}{\exp\left(-K_E \frac{n_p e^2}{akT} \right)} = \int_0^t \pi a^2 \bar{c}_i N_i \mathrm{d}t \tag{12}$$

Thus, the average charge, n_p, caused by the diffusion charging in a time period, t, by a particle diameter d_p, can be found from Eq. (13).

$$n_p = \frac{d_p kT}{2K_E e^2} \ln\left(1 + \frac{\pi K_E d_p \bar{c}_i e^2 N_i t}{2kT} \right) \tag{13}$$

Here, d_p is the particle diameter. The above equation was initially derived by White (1951, 1963) for particles in the continuum regime, $Kn \ll 1$. It was shown later that the model is only valid for the free molecular regime, $Kn \gg 1$ (Gentry and Brock, 1967; Liu *et al*., 1967a). However, its inability to take into account the image force effect can result in significant errors (Brock, 1969, 1970). In a later work, Liu *et al*. (1967a) modified White's equation, taking into account the curvature of the ion trajectory resulting from the electrical charge on the particle. Gentry and Brock (1967) solved Boltzmann's collision equation and confirmed the validity of White's equation. They further pointed out that the equation applies only when $Kn \to \infty$. However, the use of the Boltzmann distribution for determining the spatial distribution of ions had some drawbacks. Fuchs and Sutugin (1971) suggested that, due to the lack of ion-neutral molecule collision in the vicinity of the particle, the Boltzmann distribution was not obtained. They suggested that the derivation of Keefe *et al*. (1959) was better. According to the approach of Keefe *et al*. (1959), the trajectories of ions in the force field created by the particle charge were considered. Pui (1976) later integrated the ion flux expression given by Keefe *et al*. (1959) and showed that their equation gave identical results to White's equation for the case of unipolar diffusion charging.

UNIPOLAR NANOPARTICLE CHARGER DEVELOPMENTS

A number of unipolar nanoparticle charger designs have been developed and presented in the literature. Depending on the mechanisms used to generate the ionized gas, the chargers can be classified as: (i) a corona discharge charger, (ii) a radioactive charger, and (iii) a photoelectric charger. The following paragraphs give a brief review of the different designs of these chargers and a comparison based on the reported $N_i t$ product and charging efficiencies.

Corona Discharge Chargers

Corona discharge is among the most common techniques to produce high ion concentrations and there have been numerous extensive studies in the past (Hewitt, 1957; White, 1951, 1963; Liu *et al.*, 1967b; Liu and Pui, 1975; Pui, 1976). The phenomenon is used in many industrial applications such as electrostatic coating and

precipitation (Lawless and Sparks, 1988). Electrostatic charging by the corona dischargers is also commonly employed in determining aerosol size distribution by electrical mobility analysis. Corona discharge is produced by a nonuniform electrostatic field such as that between a needle and plate or a concentric wire and a tube. Air and other gases can undergo electrical breakdown when the electric field strength is high. For the case of the wire and the tube, the only place this breakdown can occur is in a very thin layer at the wire surface. In this corona region, electrons have sufficient energy to knock an electron from gas molecules creating positive ions and free electrons. During this process, aerosol flow is directed across the corona discharge field and is charged by random collisions between the ions and particles due to Brownian motion of ions in space. For particle diameters larger than 1 μm, field charging also takes place. The amount of ion deposition on the particle surface depends on resident time, particle radius and shape, electric field, etc. This technique has been applied successfully and several designs of aerosol corona charger have been employed and described in the published literature (Intra and Tippayawong, 2009), both corona-wire and corona-needle chargers. Therefore, an ideal unipolar corona discharge charger would have high ion concentrations in the charging zone with no or a low strength electric field.

In the corona-wire charges, Hewitt (1957) was one of the first to develop and investigate experimentally a corona-wire diffusion charger to examine the charging process in electrostatic precipitators. The charger consisted of a cylinder with a concentric corona wire placed along the axis, attached to the inner surface of the cylinder. A small path was formed to carry the aerosol flow. The main corona discharge volume and the aerosol flow region were separated by a metallic mesh, and an alternating voltage difference was applied between this mesh and the outer electrode of the charger to reduce particle losses. In his work, Hewitt (1957) conducted experiments for particles in the size range between 60 to 700 nm, and reported that the electric field strength resulted in high losses for particles with a diameter as small as 70 nm. At the same time, Penney and Lynch (1957) investigated the same process using a Hewitt's charger. Several subsequent researchers have adopted similar designs to investigate diffusion charging of aerosol particles. However, it was not until Whitby and Clark's (1966) work that the corona-wire chargers based on Hewitt's original design was employed in an electrical aerosol analyzer (EAA) for charging aerosol particles prior to electrical mobility classification.

In a later work Liu *et al*. (1967b) experimentally studied the diffusion charging of aerosol particles by unipolar ions over the pressure range of 0.0311 to 0.960 atm using monodispersed aerosols of dioctyl phthalate. In the charger of Liu *et al*. (1967b), an AC square-wave voltage was applied to the solid electrode to minimize the aerosol loss, which occurred in the charging process. An improvement on the charger of Liu *et al*. (1967b) was designed by Liu and Pui (1975) and later experimentally studied by Pui (1976) and Pui *et al*. (1988). As shown in Fig. 1, it consisted of two concentric metal cylinders with a fine tungsten wire placed along the axis of the cylinders. A positive high voltage was applied to the wire to generate a corona discharge field. The ions produced were either

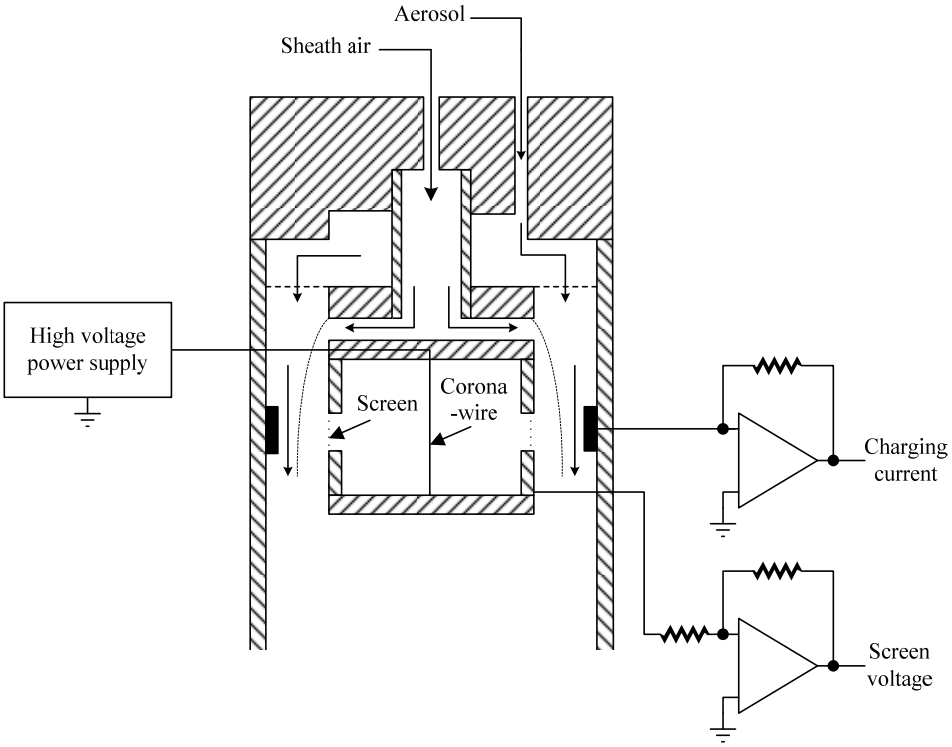

Fig. 1. Schematic diagram of the diffusion charger developed by Liu and Pui (1975) and Pui (1976).

collected by the inner cylinder or flowed through the screen opening on the inner cylinder to the annular gap space outside. In the annular gap space, the ions collided with the aerosol particles and caused the latter to become charged. In Liu and Pui (1975) charger, a sheath air flow was used adjacent to the inner cylinder in order to displace the aerosol stream away from the screen and to prevent aerosol particles from entering the high intensity corona discharge region. The authors reported that the nominal $N_i t$ product was adjustable over a range from less than 1×10^6 to over 3×10^7 ions/cm^3 s. Significant charged particle loss was found below 10 nm.

From the observation that the occurrence of small particle losses were associated with corona-wire diffusion chargers, Buscher *et al*. (1980) modified and investigated the unipolar diffusion charger of Pui (1976) by adopting the configuration of the surfaces in contact with the aerosol being entirely conductive and connected to ground, to avoid particle losses due to insulator charging, and the inlet tubes for aerosol and sheath air being designed to achieve a high particle penetration and laminar flow inside the charger. It was found that the penetration decreased towards small particles where diffusion losses were highest, and the $N_i t$ product was approximately 1.1×10^7 ions/cm^{3}s for the charger. The authors also reported that, for ion concentrations greater than 10^6 ions/cm^3, space charge had to be considered for the spatial dependence of the $N_i t$ product.

Hutchins and Holm (1989) constructed and tested an aerosol charger using sinusoidally driven ion current from a corona discharge. This charger utilized a continuous corona discharge from fine wires located in cylindrical cavities in opposite walls of a rectangular aerosol flow channel. A 3000 Hz AC voltage with maximum amplitude of 10 kV was applied across the channel gap to produce an ion current which reversed direction with the cycling of the electric field. Aerosol particles moving through the channel were impacted by unipolar ions from first one side and then the other. Lateral motion of charged particles was oscillatory at the frequency of the applied electric field. This served to minimize loss of charged particles due to wall deposition. It was reported that the particle charge levels calculated were in satisfactory agreement with measured particle charges.

A new type of high volume electrostatic charger was proposed by Cheng *et al.* (1997). This corona charger was developed for charging aerosols having flow rates of 0.6–6.0 m^3/s. Fig. 2 shows a schematic diagram of the high volume electrostatic charger. It had the configuration of annulus flow parallel to the charging wire. The corona charging was accomplished by six wires which were mounted around a Teflon rod holder and maintained at a high electric potential (> 5 kV). Transpiring air was used to minimize the electrostatic particle losses. The authors reported that deposition of charged particles in the submicron size range in the charger can be substantially reduced by using a transpiration flow rate of 2.4 m^3/s or greater.

A similar design concept to the charger of Pui (1976) has also been used in the unipolar charger of Kruis and Fissan (2001). In this design, shown schematically in Fig. 3, the particle-laden gas is introduced via a short inlet section into a square charging zone. The charging zone of this charger is separated from the two ion production zones by means of metal wire screens to prevent the expansion of the aerosol flow into the corona discharge zone. These wire screens are connected to two square-wave generators of opposite phase and a maximal voltage difference of 600 V. The bottom and top of the charging zone are composed of isolating material. Positive ions are produced by corona discharge of Au wire placed in the center of a metal cylinder. It was reported that there exists an optimal length of the charging channel for each gas flow rate through the charger, which minimizes losses of charged particles, while simultaneously having a sufficiently large $N_i t$-product and high extrinsic charging efficiencies.

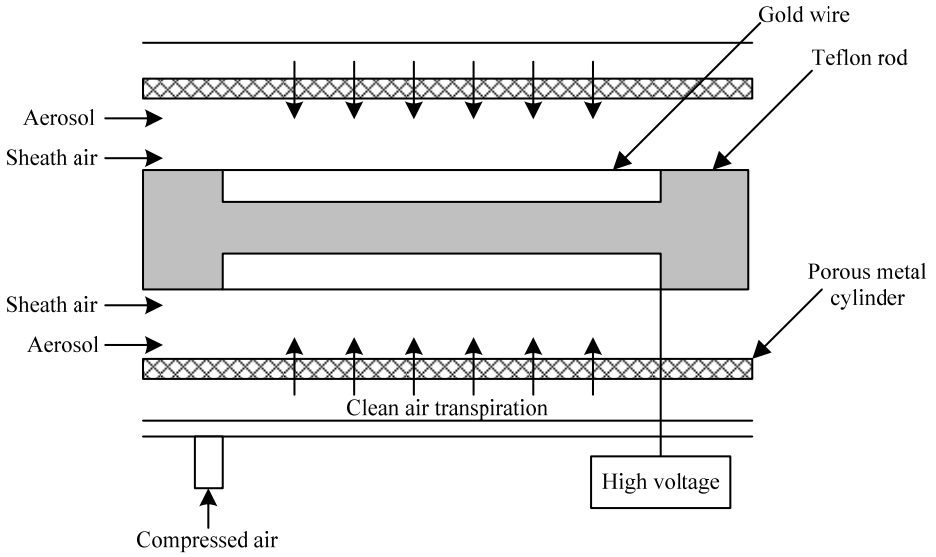

Fig. 2. Schematic diagram of the high volume electrostatic charger developed by Cheng *et al*. (1997).

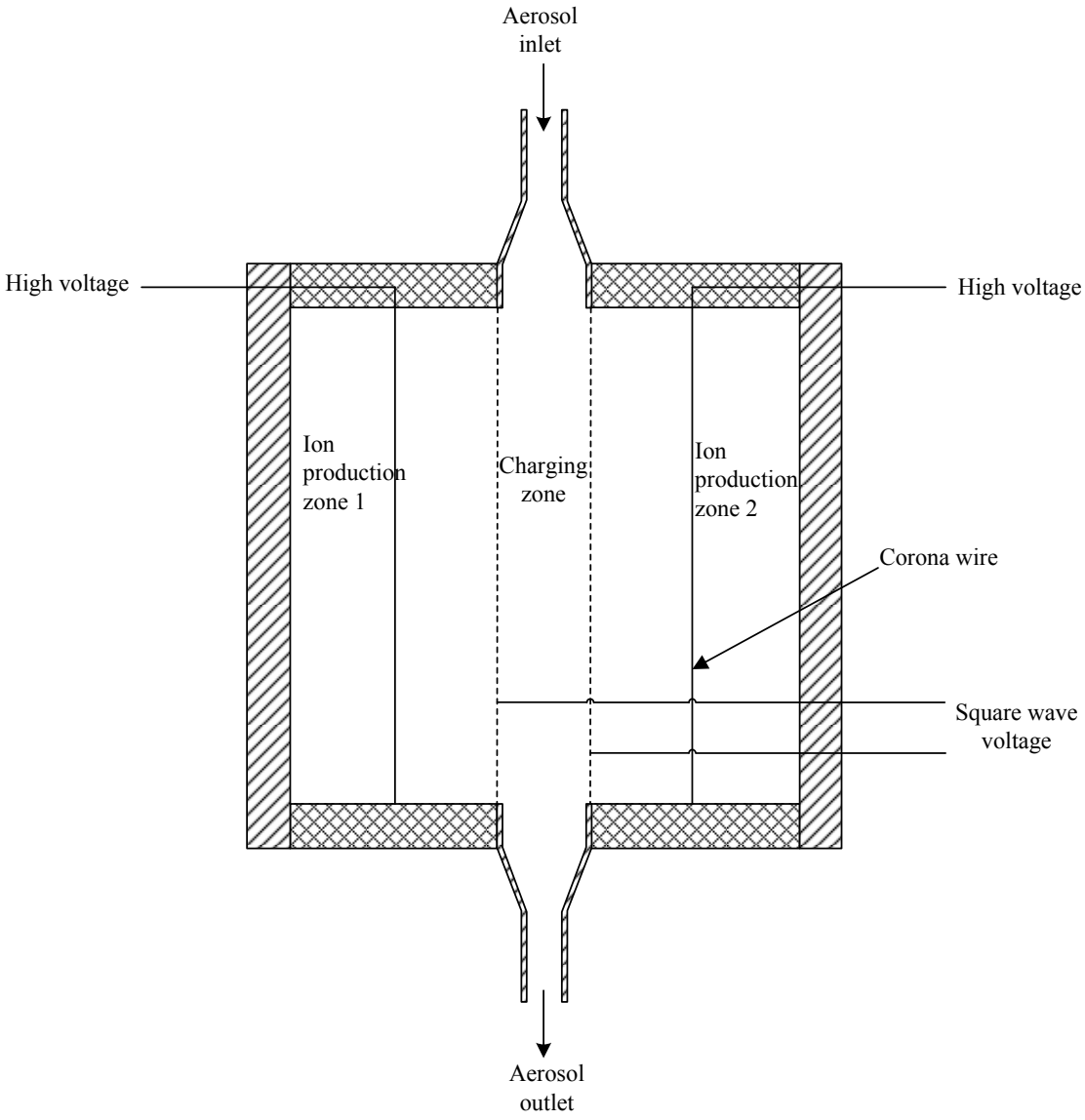

Fig. 3. Schematic diagram of the twin Hewitt charger developed by Kruis and Fissan (2001).

A newly designed Hewitt-type corona charger was proposed and investigated by Biskos (2004) and Biskos *et al*. (2005a, 2005b). As shown in Fig. 4, it consisted of two concentric electrodes with a corona-wire placed along the axis. A tungsten wire maintained at a positive high voltage was used to produce the corona discharge, while the generated ions migrated to the inner electrode due to the high electric field in the region. The inner electrode was made of a metallic mesh in order to allow ions to flow in the charging zone. An AC voltage applied on the outer electrode forced ions to enter the charging region without causing charged particles to precipitate on the charger walls, while the perforated inner electrode was connected to ground. The inner electrode maintained a laminar flow of the aerosol stream, which was highly desirable for achieving a uniform residence time of the particles. Sheath air flowed in the ion generation area so that the axial pressure gradient of the aerosol and sheath flow streams were the same. The aerosol flow passed through the annulus formed by the two cylinders, where the active charging region had a total length of 60 mm. The authors reported that neglecting the space charge effect can lead to significant errors when the ion concentration in the charger is greater than 5×10^{13} ions/m^3.

Another type of unipolar corona-wire charger designed for use without sheath air has also been recently proposed by Unger *et al*. (2000, 2004) and later studied by Intra and Tippayawong (2005). It consisted of a coaxial corona-wire electrode placed along the axis of a metallic cylinder. A DC high voltage is used to produce the corona discharge on the wire electrode while the outer metallic cylinder is grounded. In the work, a semi-empirical method to determine the electrostatic characteristics of the diode type corona aerosol charger based on ion current measurement and electrostatic charging theory was presented. It was reported that the results from a mathematical model were in agreement with those from experimental investigation of the charger, and that the space charge effect was significant

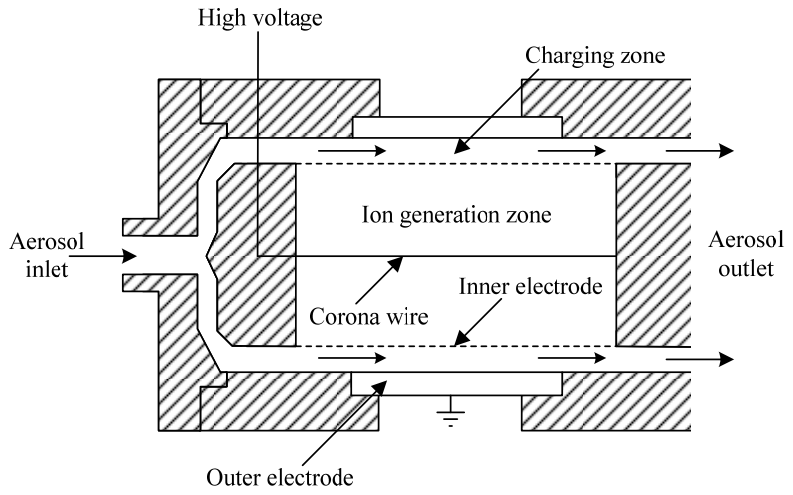

Fig. 4. Schematic diagram of the unipolar corona-wire diffusion charger developed by Biskos *et al*. (2005a).

and must be taken into account at high ion number concentration and low flow rate.

In the corona-needle chargers, Whitby (1961) developed the first needle-type corona charger as shown in Fig. 5, which was capable of converting the corona current into free small ions with 100% efficiency. It consisted of an arrangement of a sharp needle held at high potential upstream of a small sonic orifice to generate the ions within a non-conductive housing. Clean air entered at the inlet and then passed through the orifice plate. Positive, negative, or alternating current voltages on the needle electrode with respect to the orifice plate were used to produce positive, negative, or a mixture of positive and negative ions. It was reported that the ion generator produced unipolar or a mixed positive and negative ion concentration of up to 10^{11} ions/cm^3 in the charging zone, and total ion outputs of 10^{14}/s.

Jaworek and Krupa (1989) proposed a unipolar charger design to improve the particle losses without sheath air by adopting on AC electric field. Their charger consisted of parallel needle electrodes. Each needle is connected to a high voltage DC source. Between these electrodes, two grids made of brass rods 3 mm in diameter spaced about 15 mm were located. The windings of the transformers were arranged in such a manner that opposite sign of potential of each grid was obtained at the same half-period. The amplitude of the applied sinusoidal-waveform AC voltage was lower than the potential of each corona electrode to enable emission. Particles passing through the charger are not precipitated on any electrodes, but undergo only oscillations with a small amplitude. It was reported that the charging efficiency is maximum for the AC filed frequencies of about 300 Hz and space charge density in the charging zone of 0.2 mC/m^3. The charging time was about 50 ms.

A new corona jet charger shown schematically in Fig. 6 was proposed by Medved *et al*. (2000). It was currently employed by the TSI 3070A electrical aerosol detector (TSI, 2004b). Ions were generated at a corona needle tip located in a small ion-generation chamber which was connected to a mixing chamber via an orifice. The chamber was isolated from a field-free mixing chamber where the aerosol was exposed to the ions. An air flow transferred the ions into the mixing chamber, and an opposing aerosol flow promoted mixing of the aerosol and the ions. The design created turbulent conditions in the mixing chamber.

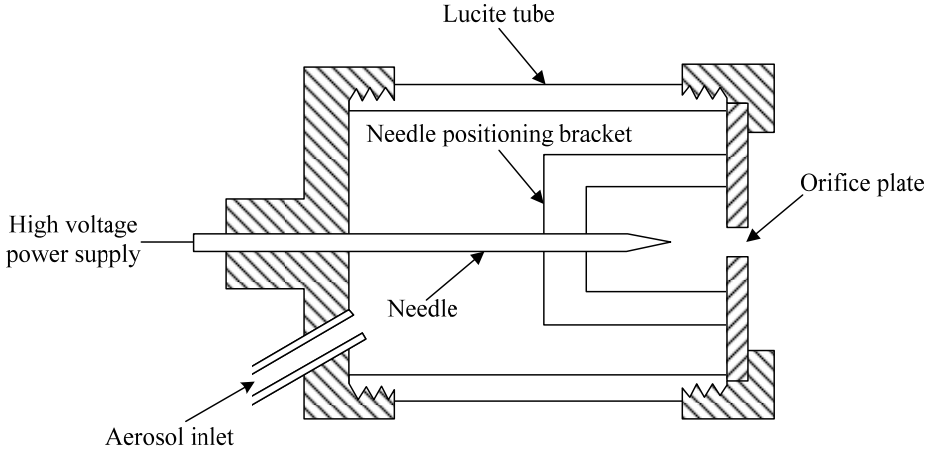

Fig. 5. Schematic diagram of the sonic jet ion generator developed by Whitby (1961).

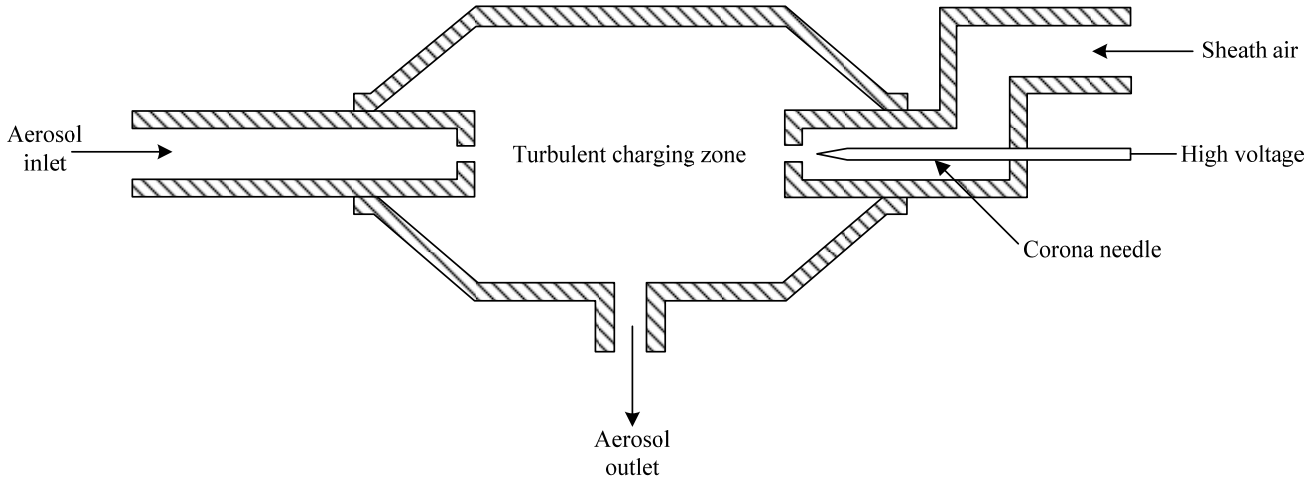

Fig. 6. Schematic diagram of the corona jet charger developed by Medved *et al*. (2000).

Since the aerosol-ion mixture was not subjected to an applied electric field, the only field negligible was one from the ion space charge itself. It was reported that particles were more efficiently charged, compared to corona-wire chargers due to better turbulent mixing.

To further improve the design concept of the Medved *et al*. (2000) charger, Marquard *et al*. (2006) designed and investigated a twin corona-needle charger. It was a twin corona module charger, shown schematically in Fig. 7, consisting of a cubic chamber made of polyethylene with two charging modules placed on opposing side walls perpendicular to the main flow. Within these modules, ions were generated in a point-ring corona configuration based on the ion gun concept of Whitby (1961), and transported by humidified air through the ring into the particle charging chamber. Inside the charger, additional metallic plates were placed around the corona module holes. Particle residence times were between 3 and 10 s, and dilution ratios resulting from the corona flows were $1.1 < f < 1.9$. The authors reported high charging efficiencies for sub-100 nm particles.

A simple corona-needle charger without sheath air capable of high efficiency unipolar charging of nanometer-sized particles (30% for 10 nm particles) was proposed by Hernandez-Sierra *et al*. (2003). Alonso *et al*. (2006) later

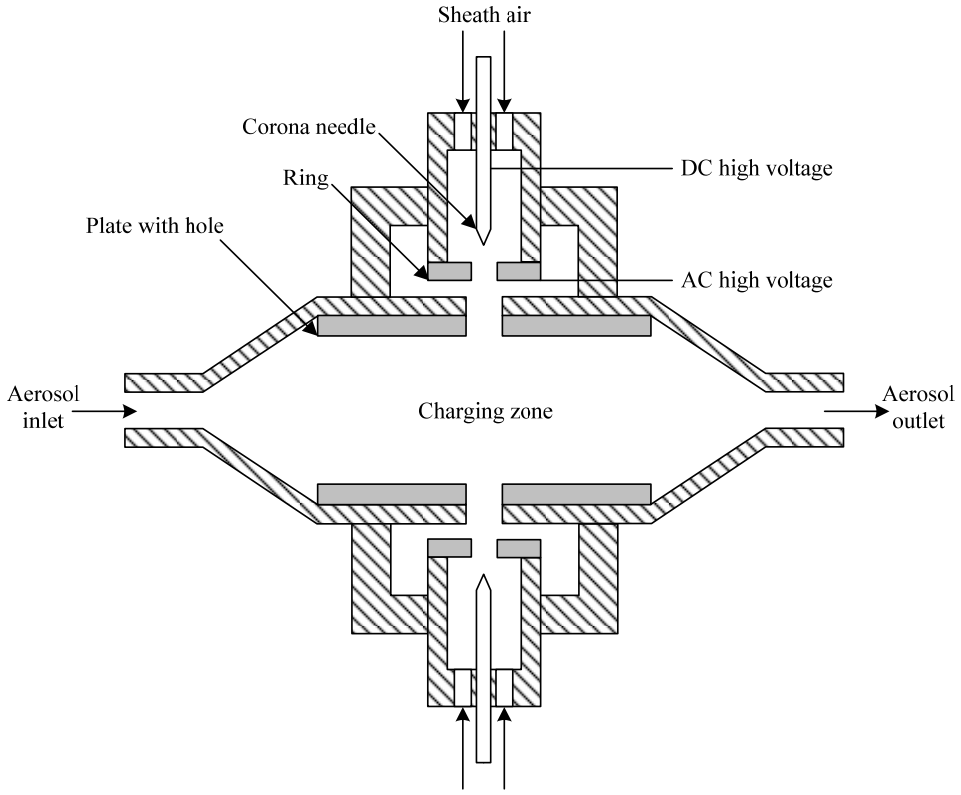

Fig. 7. Schematic diagram of the twin corona module charger developed by Marquard *et al*. (2005).

proposed a design to improve the performance of Hernandez-Sierra *et al.* (2003) charger by modifying aerosol inlet geometry as well as the manner in which the discharge electrode is positioned. Fig. 8 shows a schematic diagram of the newly developed corona needle charger. In the charger of Alonso *et al.* (2006), diffusion losses in the charger were about 25% for 3 nm particles and 7% for 10 nm particles. The authors reported that the attainable extrinsic charging efficiency for nanometer-sized particles is about one order of magnitude higher than that of commercially available bipolar chargers. No additional new particles are formed by the corona discharge under certain conditions.

Intra and Tippayawong (2006a, b) constructed and evaluated a corona needle charger for unipolar diffusion charging of nanoparticles. The corona needle charger geometrical configuration is similar to the ionizer used by Hernandez-Sierra *et al.* (2003) and Alonso *et al.* (2006). However, differences exist between the Intra and Tippayawong (2006a, b) and the Alonso *et al.* (2006) chargers. They include: (i) a tangential aerosol inlet to ensure uniform particle distribution across the annular aerosol entrance to the charging zone, and (ii) intended operating pressure at sub-atmospheric level. The authors also reported that particle loss inside this charger was smaller than the corona-wire charger from the previous work (Intra and Tippayawong, 2005).

To prevent precipitation or break-up of aerosol particles due to the strong electric field when passing through the charger, a so-called indirect corona charger was developed and proposed by Choi and Kim (2007). A schematic diagram of the charger is shown in Fig. 9. It consisted of two zones: an ion generation zone and particle charging zone. In the ion generation zone, positive ions were generated by corona discharge, some of which were ejected to the particle charging zone by an external electric field and ion carrier air. In the particle charging zone, the ejected ions moved to an electric plate by a weak electric field and some of them adhered to the particles surface. The corona voltage of ion generation zone and the particle charging zone. It was reported that the charge distribution of the particles were identical, except for 16.9 nm particles. Ion evaporation phenomenon of particles smaller than 40 nm in diameter was not detected.

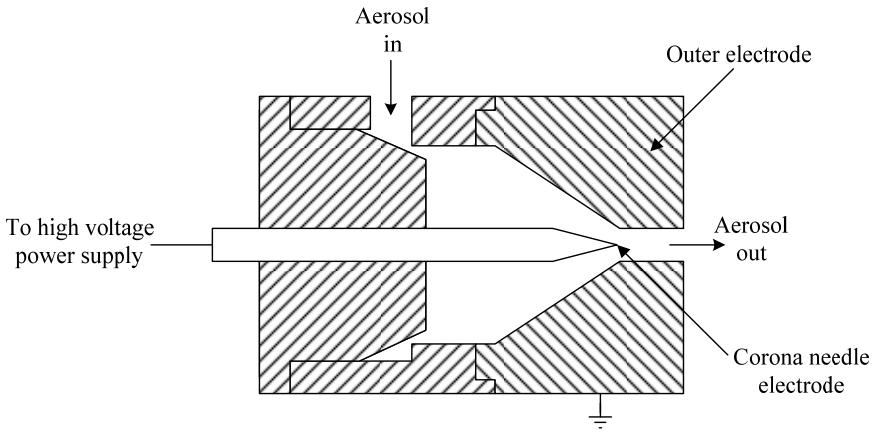

Fig. 8. Schematic diagram of the corona-needle charger developed by Alonso *et al*. (2006).

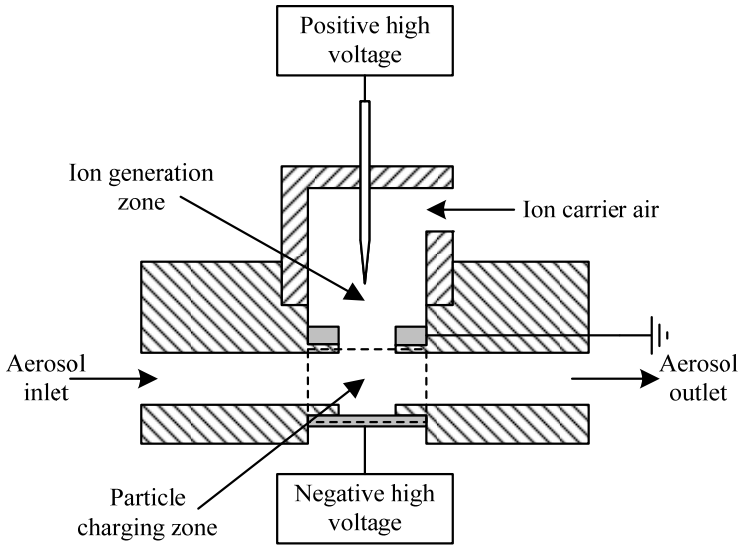

Fig. 9. Schematic diagram of the indirect corona charger developed by Choi and Kim (2007).

A newly design unipolar diffusion charger for real-time measurements of submicron particles was proposed by Park *et al.* (2007). Their charger, which was of similar concept to that by Medved *et al*. (2000), consisted of a corona discharge zone, mixing zone and ion trap zone. It was reported that the total particle losses inside the mixing and charging zones were below 15%. In a subsequent work, Park *et al.* (2009) introduced a design and performance test of a multi-channel diffusion charger for real time measurements of submicron aerosol particles having a unimodal log-normal size distribution, shown schematically in Fig. 10. It consisted of discharge, mixing and charging zones, and three flow channels for obtaining three different residence times and average charges of particles in the channels. It was reported that the estimated results for NaCl particles showed deviations of 22 % for the total number concentration and 10 % for the geometric mean diameter and the geometric standard deviation.

Alternatively, Kwon *et al*. (2007) developed a unipolar charger for nanoparticles by the surface-discharge microplasma. Fig. 11 shows a schematic diagram of the surface-discharge microplasma aerosol charger (SMAC). The unipolar ions were generated by the surface discharge of a single micro-structured electrode located on a dielectric barrier sheet by applying DC pulse. Penetration and charging were carried out for nanoparticles in the size range of 3 to 15 nm. The authors reported that more than 90% of inlet nanoparticles penetrated the charger (less than 10% of particles were lost) without the use of sheath air. It was also shown that the measured charging efficiencies agreed well with the diffusion charging theory.

A unipolar mini-charger for a personal nanoparticle sizer was proposed by Qi *et al*. (2008), as shown in Fig. 12. In this work, the extrinsic charging efficiency of the prototype mini-charger was optimized for different aerosol flow rates. Both intrinsic and extrinsic charging efficiencies of the prototype mini-charger at the optimal operational conditions were evaluated for particles in diameters ranging from 10 to 200 nm. It was reported that the intrinsic charging efficiency of the prototype can reach 100% at 20 nm for the 0.3 L/min flow rate, and 45 nm for the 1.5 L/min flow rate. The higher intrinsic charging efficiency at low flow rate is due to the longer residence time of particles in the device. The extrinsic charging efficiency is, however, higher for the 1.5 L/min flow rate than for the 0.3 L/min flow rate as a result of charged particle loss in the prototype.

Park *et al.* (2010) designed and evaluated the performance of a micromachined unipolar charger in terms of particle loss and charging characteristics. The fabrication of the bottom plate began by patterning a 1 mm-thick thermally-grown silicon oxide layer on a 4 in silicon wafer having $\langle 100 \rangle$-crystalline plane. In this work, the corona starting voltage of about 1.5 kV and the estimated N_i for 2 to 3.5 kV of applied voltage was within 6.5×10^6 to 4.3×10^7 ions/cm^3. It was reported that the particle losses of the charger were below 16.6 %. The number concentrations and the geometric mean diameters were estimated using a

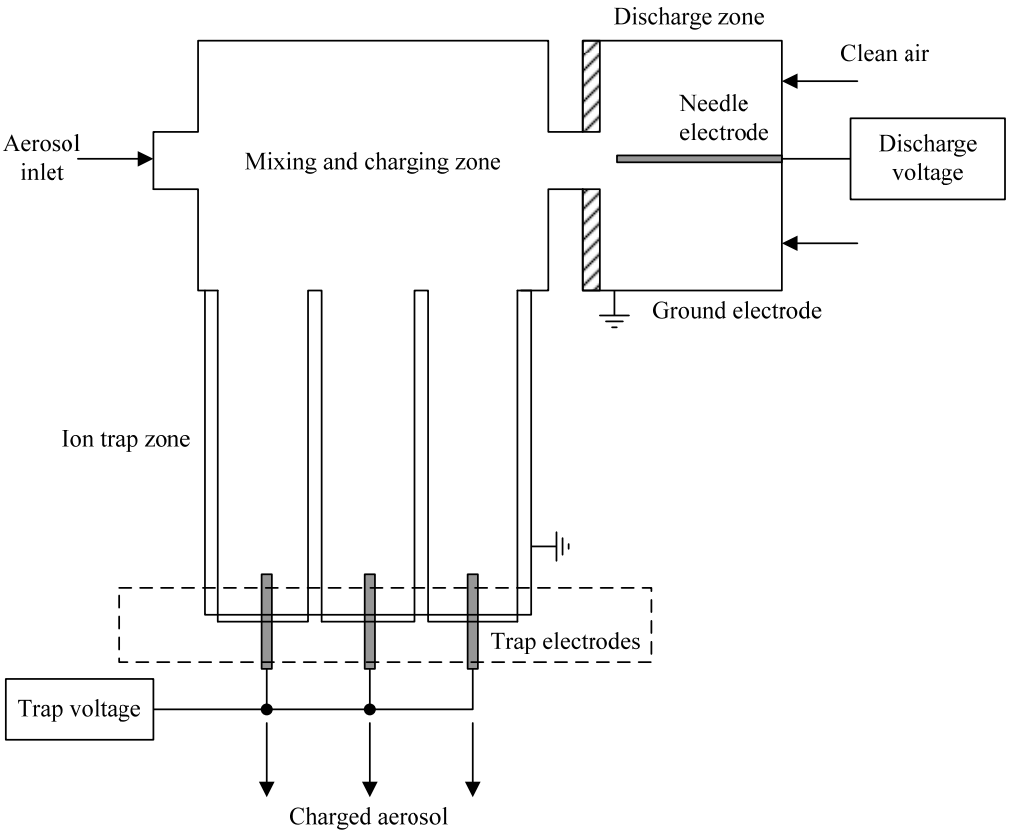

Fig. 10. Schematic diagram of the unipolar diffusion charger developed by Park *et al*. (2007).

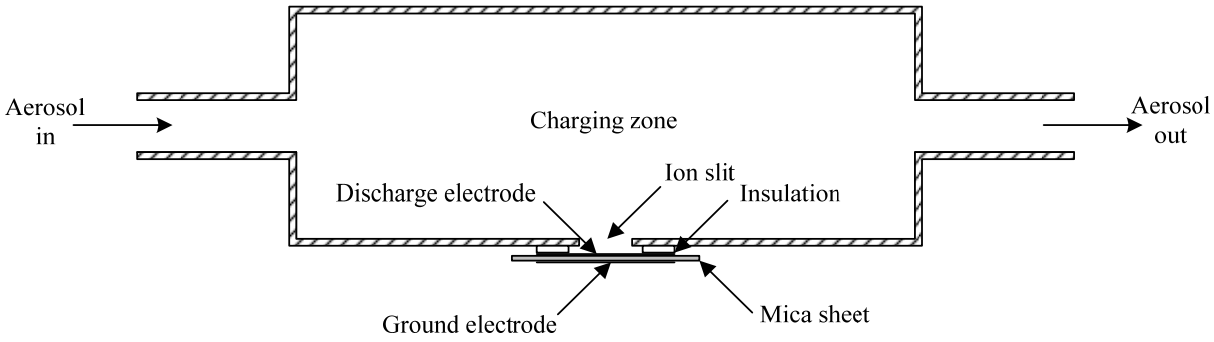

Fig. 11. Schematic diagram of the surface-discharge microplasma aerosol charger (SMAC) (Kwon *et al*., 2007).

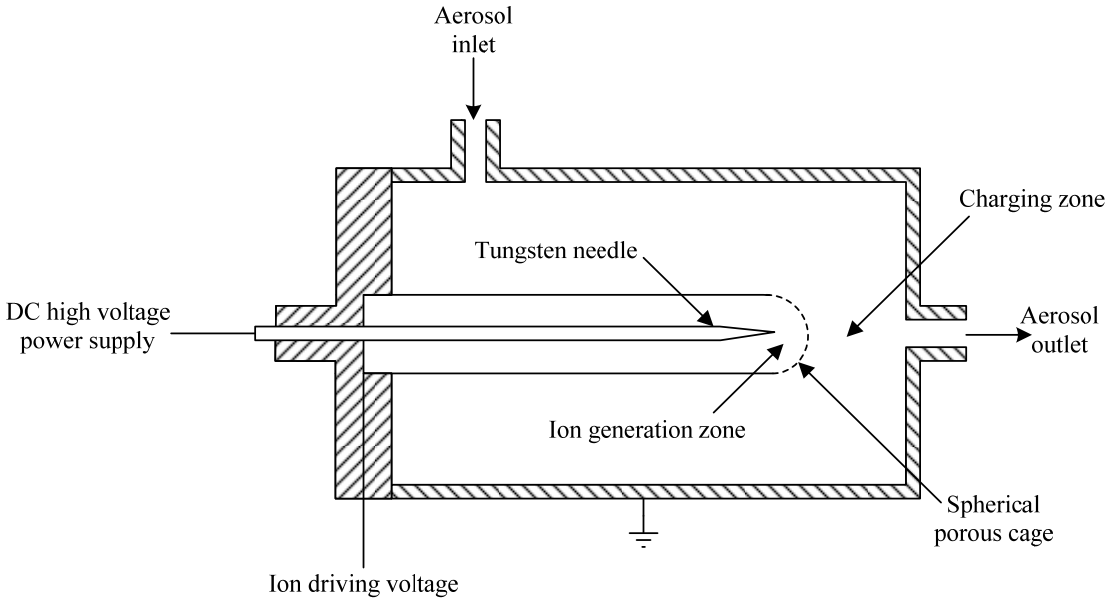

Fig. 12. Schematic diagram of the unipolar mini-charger (Qi *et al*., 2008).

method presented in Park *et al.* (2007). It was also reported that the measured data of particle loss, average particle charge, number concentration, and geometric mean diameter were in good agreement with the numerical results.

To further improve the design concept of the corona-needle ionizer of Intra and Tippayawong (2006a, b), Intra and Tippayawong (2010) later experimentally characterized the electrostatic discharge in terms of current-voltage relationships of the corona ionizer. The effects of discharge electrode cone angle and air flow rate were presented. It was reported that the charging current and ion concentration in the charging zone increased monotonically with corona voltage. Conversely, discharge currents decreased with increasing angle of the needle cone. The negative corona was found to have higher current than the positive corona. At higher air flow rates, the ion current and concentration were found to be relatively high for the same corona voltage. The effect of air flow rate was more pronounced than the corona voltage. It was also shown that the ion penetration through the ionizer decreased with increasing corona voltage, and increased with increasing air flow rate. The highest ion penetration through the ionizer of the 10° needle cone angle was found to be about 95.1 and 7.8% for positive and negative coronas, respectively. The highest ion penetration for the needle cone angle of 20° was found to be 46.3 and 4.7 % for positive and negative coronas, respectively.

Recently, Tsai *et al.* (2008, 2010) developed and investigated a unipolar charger with multiple discharging wires to enhance the extrinsic charging efficiency of nanoparticles by using sheath air near the wall of the charger, as schematically shown in Fig. 13. The charger has an inner Teflon core to fix four gold wires of 25 μm in diameter and 26 mm in length. Because the length of wires was too long which may result in high charged particle loss, the Teflon tube was used to cover unnecessary length of wires. Hence, the effective length of the wires was cut down to 15 mm to reduce the possible particle loss and deposition. In this charger, the applied positive voltage of the charger ranged from 4.0 to 10 kV, corresponding to corona current from 0.02 to 119.63 μA. Monodisperse NaCl particles of 10 to 50 nm and Ag particles of 2.5 to 10 nm in diameter were produced to test the performance of the charger with multiple discharging wires and to investigate the particle loss at different sheath flow rates, corona voltages and sheath air velocities. It was reported that the optimal efficiency in the charger was obtained at 9

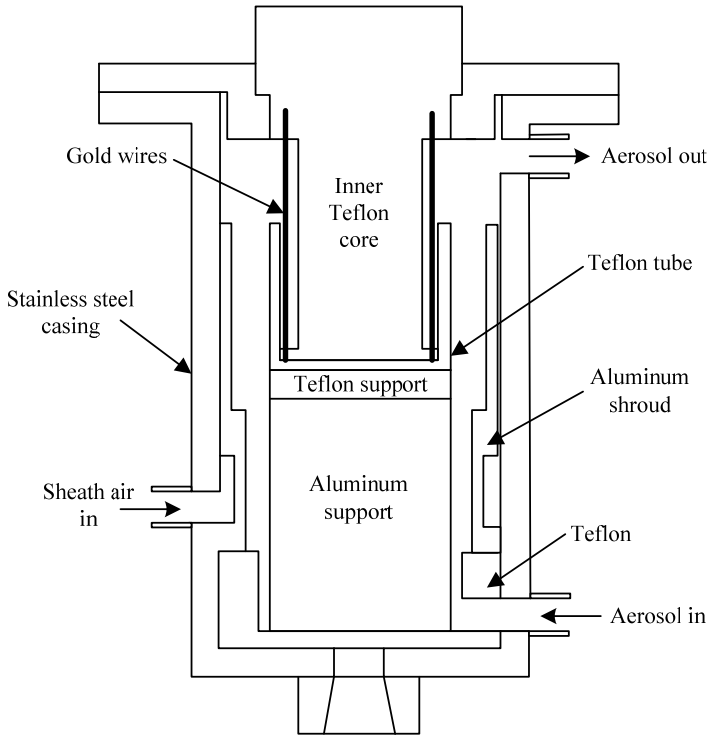

Fig. 13. Schematic diagram of the multiple discharging wires charger (Tsai *et al.* 2010).

kV applied voltage, 10 L/min aerosol flow rate and 20 L/min sheath air flow rate. The extrinsic charging efficiency increased from 2.86% to 86.3% in the charger as the particle diameter increasing from 2.5 to 50 nm.

Table 1 summarizes different designs of the unipolar corona aerosol charger for nanoparticles reported. The charger performance depends on the extrinsic charging efficiency. The extrinsic charging efficiency is a function of particle size, corona voltage, and aerosol flow rate. The extrinsic charging efficiency increases with particle diameter and decreases with aerosol flow rate. Typically, the corona discharge used in a charger have poor charging efficiencies in the ultrafine particle size range ($d_p < 20$ nm) due to high particle losses. The high ion concentration needed for efficient diffusion charging requires a high electric field to charge aerosol. A fraction of the particle losses is unavoidable in unipolar diffusion chargers. Works towards improving the performance of these chargers by reducing particle losses inside the chargers has been ongoing. These include (i) the introduction of surrounding sheath air flows at the boundary between the aerosol stream and the wall to allow more space for the charged particles to follow in random paths without precipitating on the charger walls (Liu and Pui, 1975; Pui, 1976; Buscher *et al.*, 1980; Cheng *et al.*, 1997; Kruis and Fissan, 2001; Biskos, 2004; Biskos *et al.*, 2005a, b), (ii) use of a turbulent jet of unipolar ions in a mixing chamber (Medved *et al.*, 2000; Marquard *et al.*, 2005; Choi and Kim, 2007; Park *et al.*, 2007; Park *et al.*, 2009; Tsai *et al.* 2008, 2010), (iii) application of an AC or square wave voltage to the electrode instead of DC voltage (Liu *et al.*, 1967b; Buscher *et al.*, 1980; Hutchins and Holm, 1989; Kruis and Fissan, 2001; Biskos *et al.*, 2005a, b). The AC voltage was shown to produce high charging efficiencies due to lower particle losses. Additionally, aerosol charging is a function of the ion concentration, N_i, and the mean residence time of the particles to the ions, t. For this reason, a well-designed corona charger should provide a stable $N_i t$ product that can be accurately determined for any given operating conditions.

Ionizing Radiation Chargers

Ionizing radiation is another commonly used technique to produce ions for charging aerosol particles. Radioactive sources produce bipolarly ionized gases and are most commonly employed in bipolar aerosol chargers or neutralizers. Operation of unipolar chargers is made possible by applying an electric field to the chamber with a radioactive source. In the following paragraphs, some of the ionizing radiation chargers are presented briefly.

The fundamental experiment by Ehrenhaft (1925) on radioactive aerosols has not been pursued as intensively as the theories for the charging of non-radioactive aerosols. However radioactivity has important effects on aerosol charging. Experimental works by Ivanov *et al.* (1969) used Radon gas to activate a preexisting aerosol, monodisperse dibutylphthalate. The aerosol was far more concentrated than that used by Ehrenhaft (1925), and the concentrations and charge levels were measured photographically with an applied electric field. This work was notable as it suggests that a large number of secondary electrons may be produced within the particle during the decay process, giving an average number of secondary electrons of about 12 per decay, although values up to 20 were found. Further

Table 1. Comparison of different unipolar corona aerosol chargers.

Reference	Corona electrode	N_it product	Sheath air	Aerosol/ion direction	Extrinsic charging efficiency
Hewitt (1957)	Wire	n/a	NO	Perpendicular	n/a
Liu *et al*. (1967b)	Wire	n/a	NO	Perpendicular	n/a
Liu and Pui (1975)	Wire	1×10^6–3×10^7 s/cm^3	YES	Perpendicular	1.3% at 6 nm
Buscher *et al*. (1980)	Wire	1.1×10^7 s/cm^3	YES	Perpendicular	4% at 5 nm
Hutchins and Holm (1989)	Wire	n/a	NO	Perpendicular	n/a
Cheng *et al*. (1997)	Wire	n/a	YES	Perpendicular	n/a
Kruis and Fissan (2001)	Wire	1–8 10^7 s/cm^3	NO	Perpendicular	30% at 10 nm
Unger *et al*. (2004)	Wire	n/a	NO	Perpendicular	n/a
Biskos *et al*. (2005a)	Wire	3×10^7 s/cm^3	YES	Perpendicular	60% at 20 nm
Intra and Tippayawong (2005)	Wire	1.5–4×10^7 s/cm^3	NO	Perpendicular	n/a
Whitby (1961)	Needle	n/a	NO	Perpendicular	n/a
Jaworek and Krupa (1989)	Needle	n/a	NO	Perpendicular	n/a
Medved *et al*. (2000)	Needle	n/a	YES	Turbulent	40% at 10 nm
Marquard *et al*. (2005)	Needle	n/a	YES	Turbulent	n/a
Hernandez-Sierra *et al*. (2003)	Needle	n/a	NO	Perpendicular	30% at 10 nm
Alonso *et al.* (2006)	Needle	1–4×10^7 s/cm^3	NO	Circular	55% at 13.6 nm
Intra and Tippayawong (2006a)	Needle	2–8×10^7 s/cm^3	NO	Perpendicular	n/a
Choi and Kim (2007)	Needle	n/a	YES	n/a	n/a
Kwon *et al*. (2007)	n/a	n/a	NO	n/a	3% at 10nm (uncharged particles) 5–10% at 10 nm (charged particles)
Park *et al.* (2007)	Needle	1–7×10^7 s/cm^3	YES	Turbulent	n/a
Qi *et al*. (2008)	Needle	n/a	NO	n/a	20% at 10 nm
Tsai *et al.* (2010)	Wires	n/a	YES	n/a	2.86–86.3 % at 2.5–50 nm
Park *et al.* (2010)	Needle	n/a	NO	n/a	n/a

n/a: information not available.

experiments on alpha-active aerosols were performed by Yeh (1976), who measured the charges on aerosols consisting of oxides of Plutonium, with a mean radius of approximately 0.2 mm. These were neutralised in a ^{85}Kr discharger, before being allowed to charge for 30 to 120 seconds. Experiments on aerosols by Yeh *et al.* (1976) labeled with beta-activity showed a significant self-charging effect at small decay rates. These experiments were used in a purpose designed aerosol mobility spectrometer, which allowed only a small amount of ionic space charge to become established.

Adachi *et al*. (1985) developed and investigated a simple radioactive unipolar diffusion charger, as shown in Fig. 14. The upper and lower walls of the charger act as electrodes. The upper electrode is connected with the electrometer while DC voltage (900 V or 450 V) is applied to the lower electrode where the α-ray radioactive source (^{241}Am) is located. Experiments were carried out with monodisperse aerosol particles in the size range of 4 to 100 nm and it was found that the numbers of charges on the particle can be increased to higher levels by negatively charging than by positively charging, due to the higher electrical mobility of the negative ions. Good agreement of the charger's performance with Fuchs' limiting-sphere theory was reported.

In a subsequent work, Adachi *et al*. (1992) experimentally investigated the performance of a charger similar to the previous design, shown in Fig. 15. The charger consisted of a ^{210}Po radioactive source placed between two screen electrodes enclosed by a Plexiglass tube. When a positive voltage is applied to the inlet screen electrode and the outlet electrode is grounded, a uniform electric field is established between the electrodes. Negative ions are attracted to the inlet electrode, while positive ions flow to the outlet electrode. Aerosol particles are first neutralized and then charged unipolarly before they exit the charger, making the device theoretically independent of the initial charge on the incoming aerosol. It was reported that the charger gave a unit charge to 50% of the 10 nm diameter particles with 20% particle loss. High efficiency charging was obtained under low operating pressure.

In a later work, Wiedensohler *et al*. (1994) designed and developed a low loss unipolar charger for ultrafine aerosol particles. In this design shown schematically in Fig. 16, the aerosol stream enters the core region of the charging tube. Bipolar ions are generated in two boxes placed 180° apart using ^{244}Cm source while an AC field is applied between the screen opening across from each box. Unipolar ions are drawn out of the boxes into the charging zone in the center. A sheath air flow is used to surround the aerosol stream in order to prevent particles from entering the bipolar ion boxes. It was reported that charging efficiencies of 7.5% and 12.2% were obtained for 7 nm particles when applying alternating voltages of 190V and 280V, respectively.

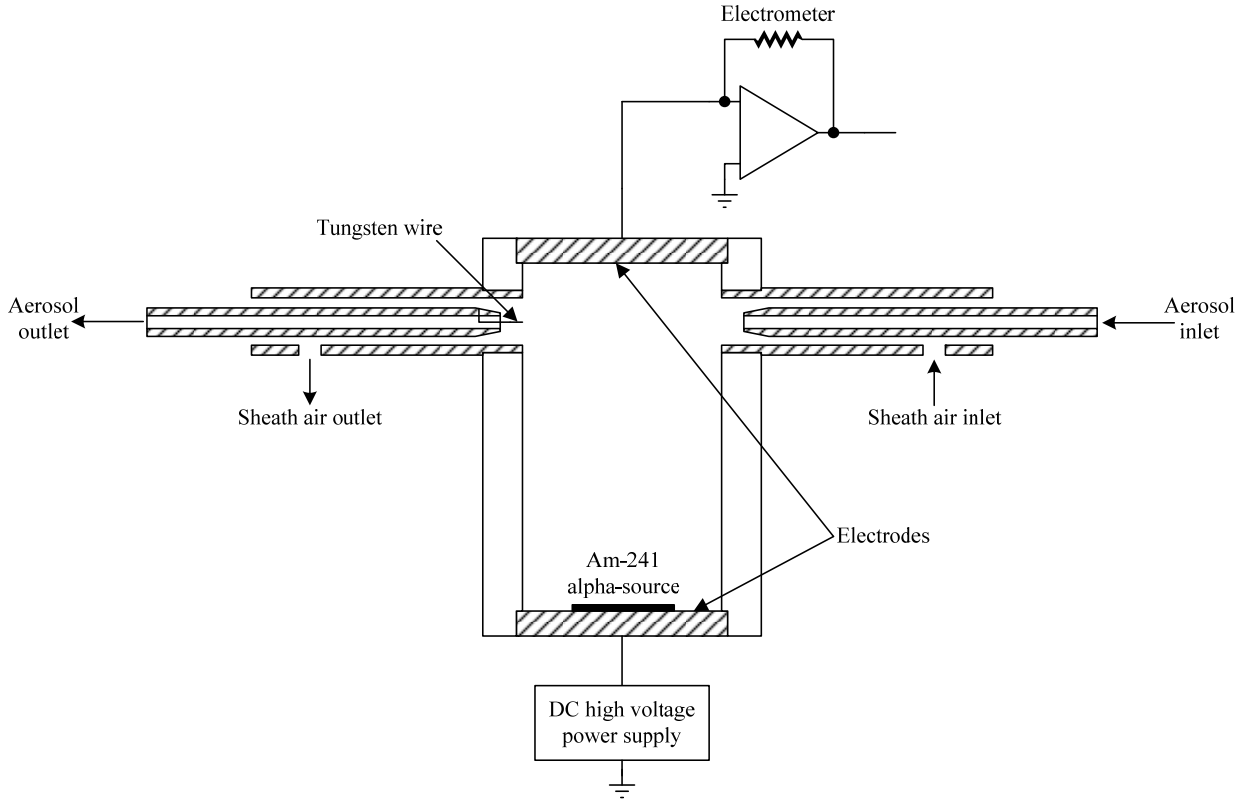

Fig. 14. Schematic diagram of the unipolar charger developed by Adachi *et al*. (1985).

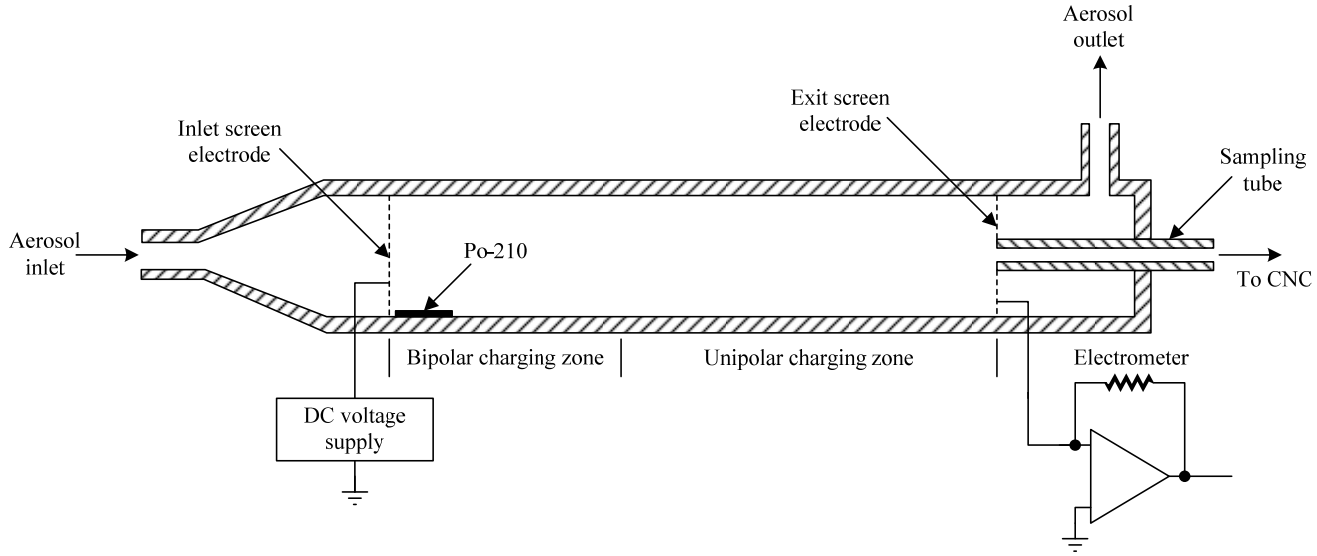

Fig. 15. Schematic diagram of the unipolar charger originally developed by Adachi *et al*. (1992).

To further improve the performance of the charger by Wiedensohler *et al*. (1994), Chen and Pui (1999) developed a high efficiency, high throughput unipolar charger for nanometer particles in the size range between 3 to 50 nm. Fig. 17 shows a schematic diagram of the high efficiency, high throughput charger, consisting of four sections: the inlet, the ion production, the unipolar charging, and the exit zones. In the inlet and ion production zones, unipolar ions are generated using ^{210}Po radioactive sources with an electric field designed to separate positive and negative ions, and to focus the selected unipolar ions into the core region of the charger. The ions with selected polarity are then attracted to the charging zone by a uniform electric field created by a series of ring electrodes applied with a linear ramped voltage. Aerosol entering the charger is sheathed with clean gas flow in order to minimize the charged particle loss. It was shown that the charger was able to achieve 90% and 95% charged particle penetration efficiency, with 22% and 48% extrinsic charging efficiency for 3 and 5 nm particles, respectively.

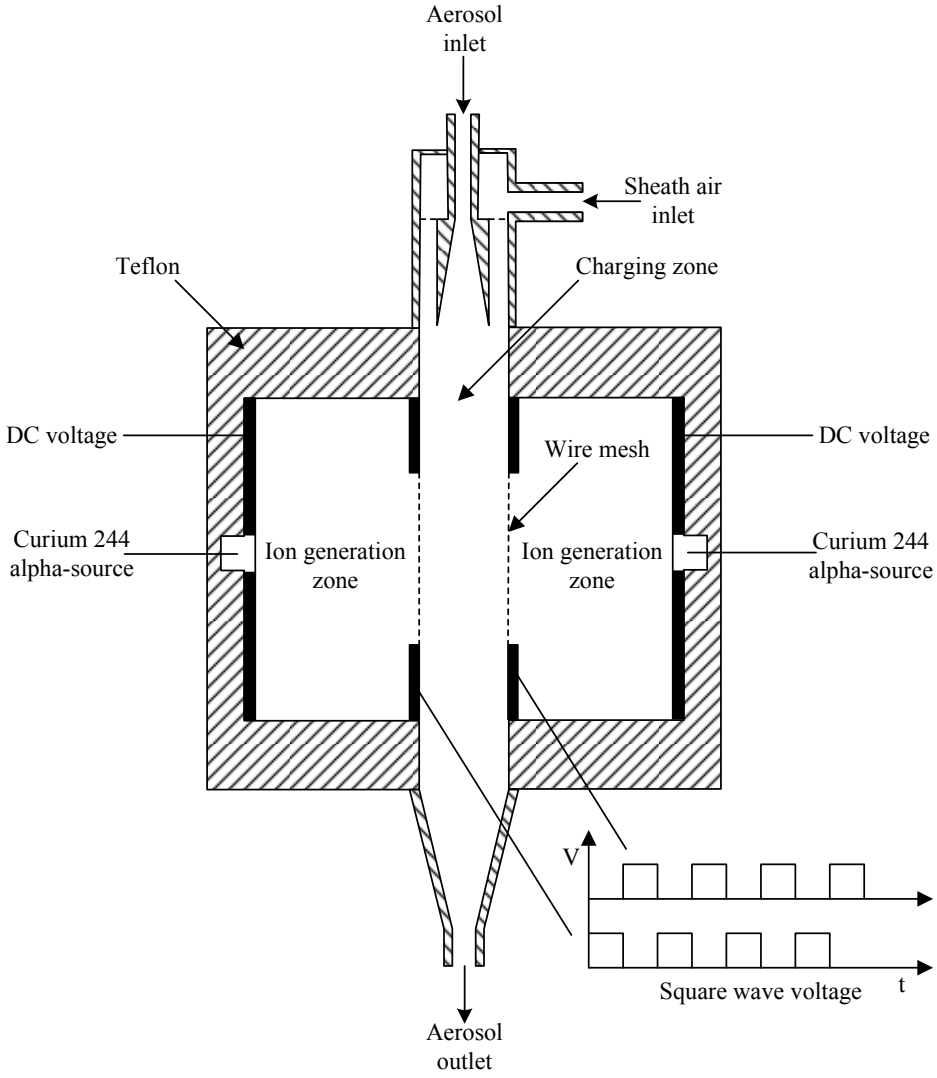

Fig. 16. Schematic diagram of the low loss unipolar charger by Wiedensohler *et al*. (1994).

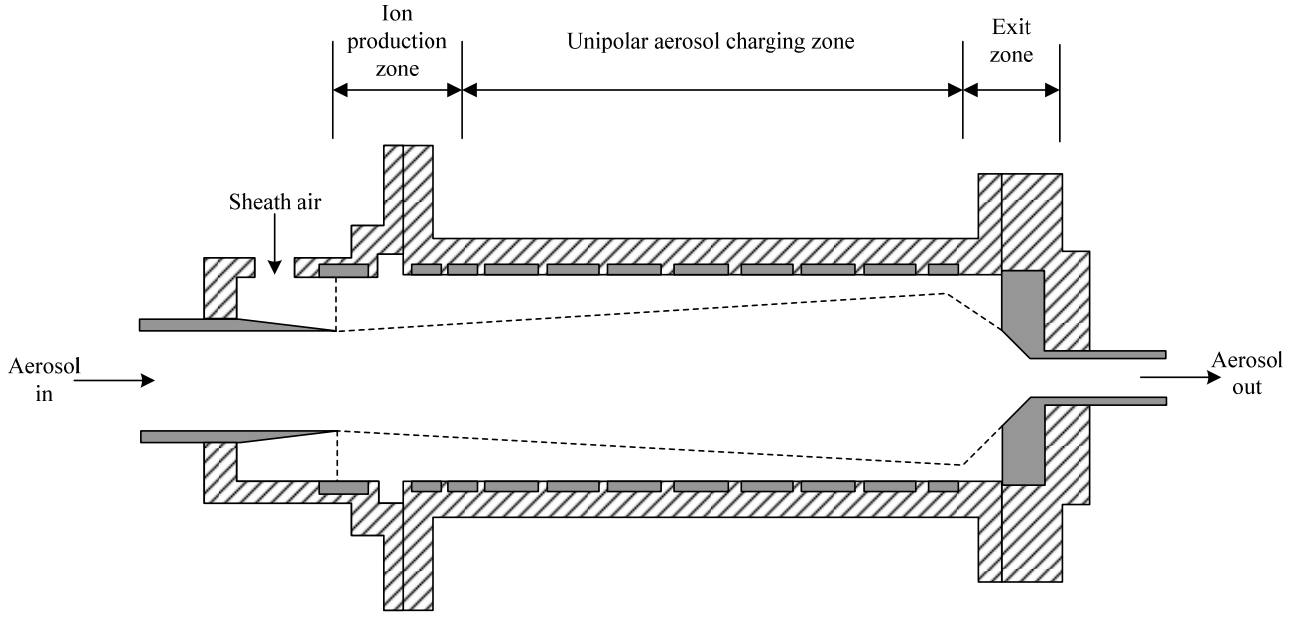

Fig. 17. Schematic diagram of the high efficiency, high throughput charger developed by Chen and Pui (1999).

The charging of fine particles in unipolar coronas irradiated by soft X-rays (3.5–9.5 keV; λ = 0.13–0.41 nm) was studied by Kulkarni *et al.* (2002). In the study, voltage–current characteristics were used to examine the corona inception voltage in presence and absence of X-ray irradiation and to estimate the ion concentrations. The capture characteristics of synthesized particles including iron oxide, sodium chloride, silica and titanium dioxide, were established in coronas, with and without X-ray irradiation. Enhanced charging of ultra fine particles in coronas was observed in conjunction with soft X-ray irradiation. The authors reported that a positive corona with X-ray irradiation resulted in the highest charging efficiencies, followed by a negative corona with X-ray, X-ray only, negative corona only and finally positive corona only.

Han *et al*. (2003) recently developed a unipolar charger for nanosized particles, based on soft X-ray photoionization. The schematic diagram of the charger is shown in Fig. 18. The emitter emits a soft X-rays below about 9.5 keV from a circular beryllium window. An X-ray beam was dispersed from the opening window of the emitter at a solid angle of about 120°. The entire charger was enclosed with a 3 mm thick PTFE container to prevent X-ray from being dispersed around. The side wall of the chamber contains a semicircular hole to admit the X-ray from the emitter into the chamber. The upper and lower walls of the chamber consist of stainless steel and act as electrodes. A DC voltage was applied to the lower wall while the upper wall was connected to ground. The bipolar ions were generated by X-ray irradiation and separated onto top and bottom plates by means of the voltage applied to the bottom electrode. Aerosol inlet and outlet ports are attached to a nonionization zone in order to induce aerosol particles to collide with completely separated unipolar ions. Their charger was found to have a higher capability for charging aerosol particles of 10 to 40 nm in diameter than the ^{241}Am charger. The charging state of particles produced by the X-ray unipolar charger was in good agreement with the unipolar diffusion charging theory, based on Fuchs' charging probability.

Table 2 summarizes the ion sources, sheath air flows, aerosol/ion direction, and extrinsic charging efficiencies of nanometer particles in the size range between 3 to 15 nm of above-mentioned unipolar ionizing radiation chargers.

Photoelectric Chargers

Photoelectric charging is derived from photoelectric effect. The phenomenon occurs when high energy electromagnetic radiation such as ultraviolet light is incident on the surface of a metal. Emission of electrons occurs from the surface of the metal, if the frequency of the incident radiation exceeds a certain threshold value. If the incident radiation is of a single frequency, the emission rate of electrons is proportional to the intensity of the radiation. However, the intensity of the radiation has no effect on the kinetic energy of the electrons emitted. There are two ways in which the photoelectric effect may be used to charge aerosols: (i) by aerosol photoemission whereby the aerosol is exposed directly to light, and (ii) by using photoelectric effect indirectly, whereby the aerosol is bathed in the electrons produced by irradiating a nearby metal. A limited number of photoelectric or UV-light studies have been investigated for aerosol particle charging. Some of the photoelectric chargers are presented in the following paragraphs.

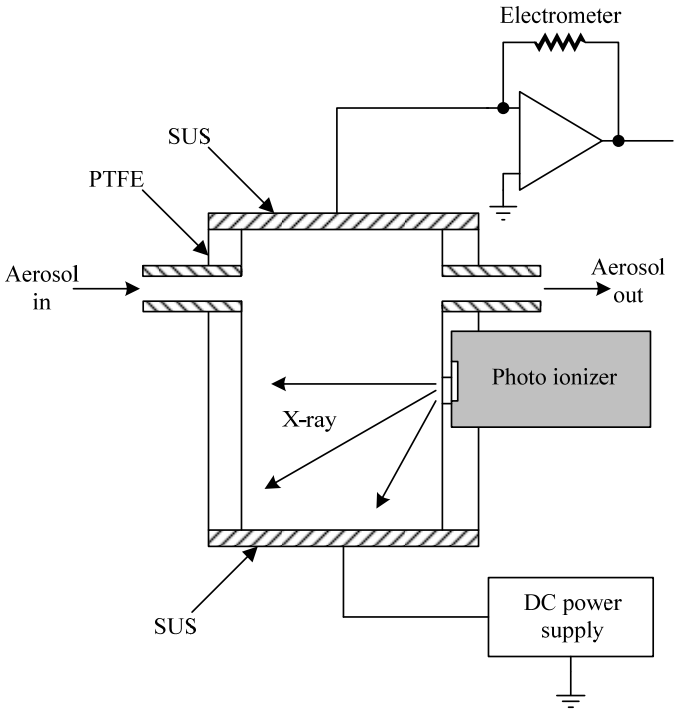

Fig. 18. Schematic diagram of the soft X-ray unipolar aerosol charger developed by Han *et al*. (2003).

Table 2. Comparison of different ionizing radiation chargers.

Reference	Ion source	Electric field	Sheath air	Aerosol/ion direction	Extrinsic charging efficiency
Adachi *et al*. (1985)	^{241}Am	DC	YES	Perpendicular	58% at 15 nm (+) 63% at 15 nm (-)
Adachi *et al*. (1992)	^{210}Po	DC	NO	Parallel	50% at 10 nm
Wiedensohler *et al*. (1994)	^{244}Cm	AC	YES	Perpendicular	7.5% at 7 nm (190 V) 12.2% at 7 nm (280 V)
Chen and Pui (1999)	^{210}Po	DC	YES	Parallel	22% at 3 nm 48% at 5 nm
Kulkarni *et al.* (2002)	X-ray	n/a	n/a	n/a	n/a
Han *et al*. (2003)	X-ray	DC	NO	Perpendicular	n/a

n/a: information not available

Schmidt-Ott *et al.* (1980) presented indirect photoelectric chargers. Aerosols are irradiated with UV-light to release electrons from the molecules on the surface of the particles. High charging efficiency for particles with a diameter less than 10 nm was reported. Burtscher *et al*. (1982) developed a device for photoelectric charging of airborne particles. The schematic diagram of the photoelectric charger is shown in Fig. 19. The light source is a Hg low pressure discharge lamp commonly used for sterilization purposes. It has an input power of 40 W and yields photons of an energy of 4.9 eV (252 nm) with an intensity of 9 W. The total photon flux is 1.14×10^{19} photons/s. It was reported that the particles generated by combustion of organic material, e.g., auto exhaust, are charged with high efficiency.

The aerosol photoemission method was adopted by Jung *et al.* (1988), with light of photon energy greater than the ionization potential of the particle which produced about 4 charges per particle (of radius 20 nm). Because of the Coulomb attraction between the emitted electron and the emitting positive aerosol particle, the ionization energy increases with every emitted electron. The apparatus has to be designed such that the build-up of space charge due to electrons was minimized.

Matter *et al*. (1995) developed the photoelectric charger for submicron aerosol particles using an excimer lamp with wavelengths between 172 and 258 nm, as shown in Fig. 20. The excimer lamp consists of two coaxial quartz glass tubes, sealed at each end. The particular gas filling used determines the wavelength of the radiation emitted by the lamp. The outer electrode was a UV-reflecting foil and the inner a UV-transparent metal mesh. The aerosol sample flowed in a quartz tube through the center of the lamp where it was strongly irradiated. Negative ions were then removed by a weak electric field (ion filter). The positively charged particles were deposited in a particle filter, where they generate an electrical current, which was measured using a current amplifier.

Bucholski and Niessner (1991) developed indirect photoelectric diffusion charging of submicron aerosol particles in clean inert gases. Monodisperse NaCl aerosols in the diameter range of 10 to 50 nm were charged by the attachment of photoelectrons emitted from different metal surfaces inside the aerosol flow duct. The metal surfaces were irradiated by UV light of 185 or 254 nm wavelength.

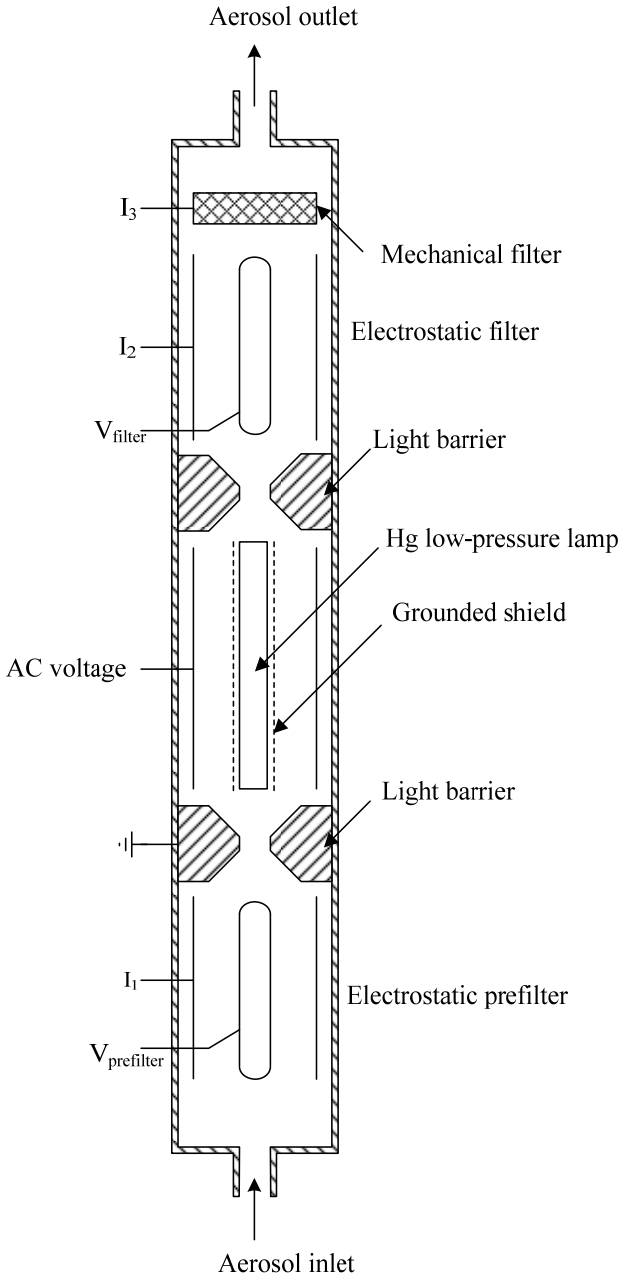

Fig. 19. Schematic diagram of the photoelectric charger developed by Burtscher *et al*. (1982).

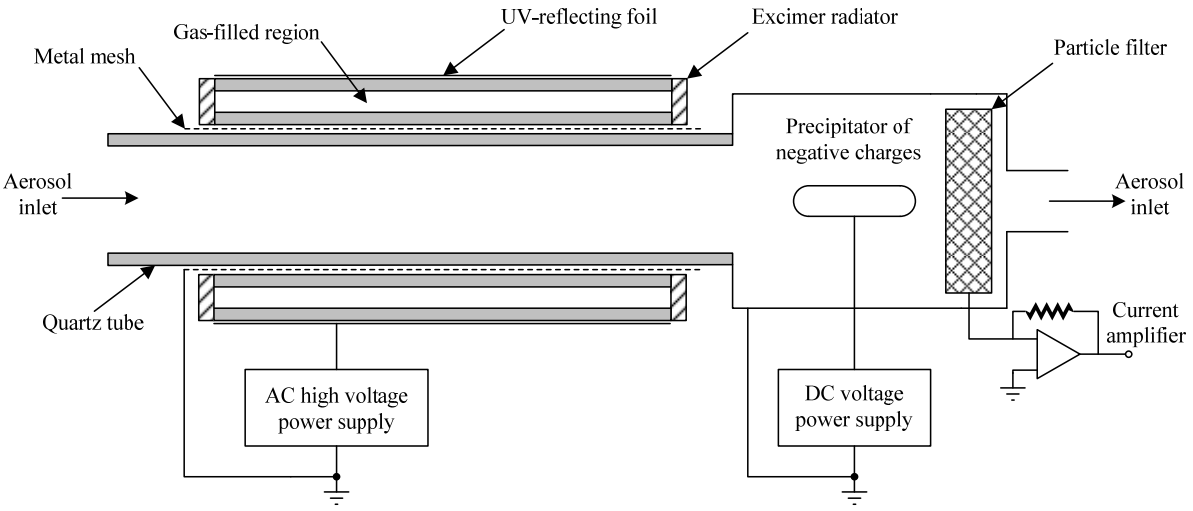

Fig. 20. Schematic diagram of the photoelectric charger developed by Matter *et al*. (1995).

The influences of particle diameter, particle number concentration, photoemitting material, electrical potential and trace compounds in the carrier gas on the charging efficiency were investigated.

Shimada *et al*. (1999) developed an airborne particle removal device using UV/photoelectrons under reduced pressure conditions. Fig. 21 shows the schematic diagram of the photoelectric particle remover. It consists of three parts connected to one another with thin, electrically insulating plastic flanges. The particles are charged and collected as they flow in the annular space between the two coaxial tubes in the middle part. The inner tube is made of quartz glass. In the inner tube, an 8 W UV lamp of 254 nm in primary wavelength is installed. The outer tube of the middle part is made of stainless steel and applied with a positive DC voltage. An electric field was formed between the annulus. Light from the lamp causes the surface of the gold film to emit a lot of photoelectrons, resulting in the production of negative ions of a high concentration in the annular space. The aerosol particles flowing in the space are negatively charged by the ions and attracted towards the outer electrode. It was found that the Fuchs' approach to ionic particle charging needs modification to predict charging of highly charged particles by ions of the same polarity. It was also shown that the removal efficiency can be increased to 100%.

Graskow (2001) designed and developed a fast photoelectric charger for nanoparticles using a KrCl excimer lamp which produces electromagnetic waves at a wavelength of 222 nm with an energy of 5.6 eV for approximately 100 ms. The schematic diagram of this charger is shown in Fig. 22. It is powered by an AC source of a ± 4 kV triangle wave pulse at a frequency of 40 kHz. The lamp is cylindrical with an internal diameter of 18 mm and a length of 120 mm. The lamp is powered through an inner electrode, while the outer electrode is grounded. The aerosol was drawn through the charging zone in a high-purity fused quartz tube concentrically aligned at the center of the excimer lamp with an inner diameter of 10 mm, and is transparent to UV light.

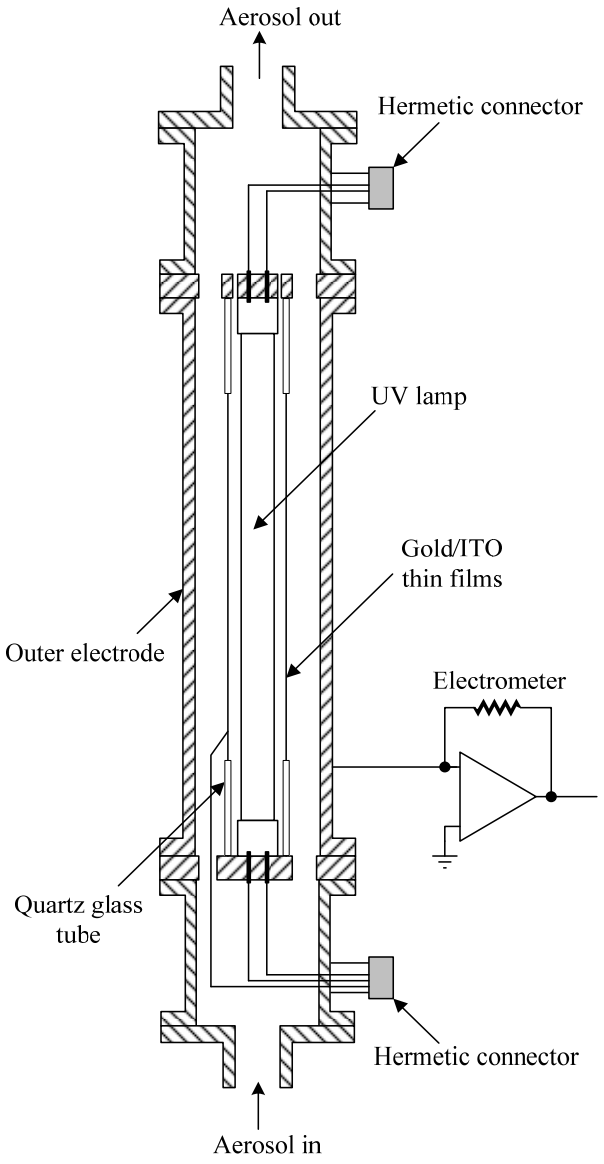

Fig. 21. Schematic diagram of the photoelectric particle removal device developed by Shimada *et al*. (1999).

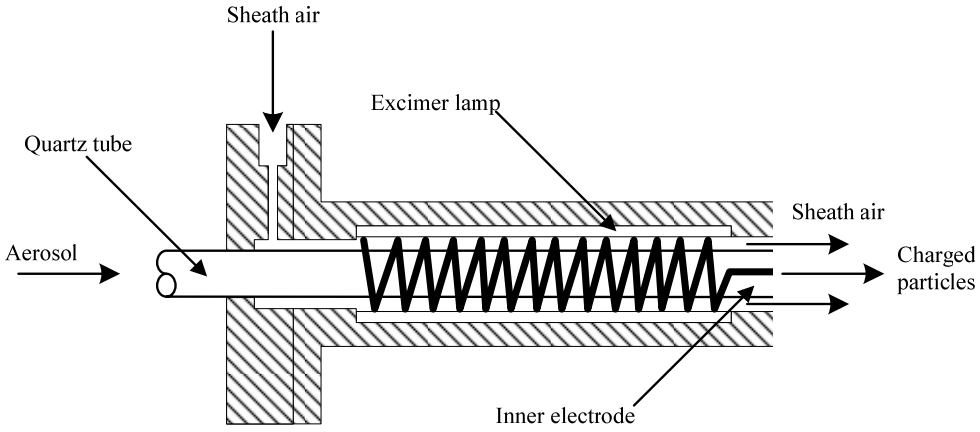

Fig. 22. Schematic diagram of the fast photoelectric charger by Graskow (2001).

Suitability of photoionization for single unipolar charging of nanoparticles at high flow rates was demonstrated by Hontañón and Kruis (2008). For this purpose, a UV photocharger has been designed, consisting of a quartz (suprasil) tube of 16 mm in diameter and 400 mm in length surrounded by three lamps of Xe excimer that emits UV light with a wavelength λ of 172 nm. In this work, the suitability of a UV photocharger followed by a DMA to deliver monodisperse nanoparticles at high aerosol flow rates has been assessed experimentally in comparison to a radioactive bipolar charger (^{85}Kr, 10 mCi). Monodisperse aerosols with particle sizes in the range of 5 to 25 nm and number concentrations between 10^4 and 10^5 1/cm^3 have been obtained at flow rates up to 100 L/min with the two aerosol chargers. It was reported that the UV photoionizer performed better than the radioactive ionizer with increasing aerosol flow rate in terms of output particle concentration. Aerosol charging in the UV photoionizer was also described by means of a photoelectric charging model that relies on an empirical parameter and of a diffusion charging model based on the Fuchs theory. The UV photocharger behaved as a quasi-unipolar charger for polydisperse aerosols with particle size less than 30 nm and number concentrations about 10^7 1/cm^3.

Other light induced charging techniques have been described, using high intensity laser pulses. These methods, such as that used by Niessner *et al.* (1988) and Kascheev and Poluektov (1991), relied on rapid heating of the aerosol and subsequent thermal ionization of the particle. The light sources, sheath air flows, wavelength, energy, and extrinsic charging efficiencies of above mentioned unipolar photoelectric chargers are summarized in Table 3.

SUMMARY

Unipolar aerosol chargers for nanoparticles can be classified according to the techniques employed for generating ions: corona discharge, ionizing radiation, and photoelectric/UV-light sources. This paper has presented an overview of development of the available unipolar aerosol chargers for nanoparticles. A brief outline focusing on the unipolar aerosol charger by corona discharge (both corona-wire and needle discharges), ionizing radiation, and photoelectric methods have been presented. It has covered the operating principles as well as detailed physical characteristics of these chargers. The main purpose of these chargers is to charge ultrafine particles (i.e. less than 10 nm) efficiently with minimal losses. This is highly desirable in electrical mobility analysis based aerosol sizing instruments, especially when electrometer current sensors are used to measure the particle number concentration downstream of the charger. However, the loss of charged particles due to electrostatic and/or space charge effects is often severe, and needs to be addressed in the development of unipolar chargers. Examples of future development are techniques involving utilization of AC electric fields and/or sheath air, modifying aerosol inlet geometry, aerosol flow direction, electrode and/or charging zone and/or ionization source direction arrangements in the existing unipolar chargers to reduce charged particle losses.

Table 3. Comparison of different ionizing radiation chargers.

Reference	Source	Wavelength	Energy	Aerosol/ion direction	Extrinsic charging efficiency
Burtscher *et al*. (1982)	Hg lamp	252 nm	4.9 eV	Parallel	n/a
Matter *et al*. (1995)	UV lamp	172–258 nm	4.95 eV	Parallel	n/a
Bucholski and Niessner (1991)	UV lamp	185, 254 nm	n/a	n/a	n/a
Shimada *et al*. (1999)	UV lamp	254 nm	n/a	Parallel	n/a
Graskow (2001)	UV lamp	222 nm	5.6 eV	Parallel	n/a
Hontañón and Kruis (2008)	UV lamp	172 nm	n/a	n/a	n/a

n/a: information not available

RECOMMENDATION FOR FUTURE WORKS

The following paragraphs provide a few suggestions for further research on both the theoretical and experimental parts of unipolar chargers for nano-aerosol.

- Further research in unipolar charger design should be focused on the particle shape effects on the unipolar diffusion charging for non-spherical particles. Most particles, such as asbestos fibers, soot aggregates, and bioaerosols are non-spherical. The shape of a particle affects the drag force, settling velocity and electrical mobility. Non-spherical particles have smaller electrical mobility than the spherical particles.
- It is well known that the electrical and chemical properties of nanoparticles itself have very strong influence on the charging efficiency. The effect of particle dielectric constant on the charging performance should be explored. Because diffusion charging is independent of particle material, it can be concluded that for particles smaller than 0.5 μm, particle material is irrelevant when considering the charging process. For larger particles, charging is dependent on the dielectric constant of the material. However, if the dielectric constant of the particle material differs significantly from calibration values, a large difference can be expected. The influence of chemical composition of nanoparticles on the charging performance should be also investigated further.
- Due to practical limitations of materials and fabrication/ assembly, further investigation should be focused on phenomena that might affect the charging performance of the chargers such as non-ideal flow or electric field, electrode eccentricity, and misalignment of various components. Computational model of flow and electric fields for ion and particle tracks should be investigated, including this effect.
- More detailed information on the properties of the ions would be of significant importance. Mass spectrometry measurements in combination with electrical mobility estimations of the ions can provide information for the whole range of ionic species in the charger. This information can then be incorporated in the theoretical and numerical models to provide more accurate predictions of the charge distribution and electrical mobility of the particles.
- A well designed corona discharge charger should provide high magnitude of ion number concentration and stability that can be accurately determined for any given operating conditions. The magnitude of the ion number concentration in the discharge zone depends, however, on the charger geometry, i.e., the distance between discharge electrode and the plane or nozzle, voltage waveform and frequency, and also on the effect of discharge electrode shape and arrangement. Further research should be focused on the influence of the discharge electrode shape and arrangement on electrostatic discharge characteristics of a corona discharge charger. It is important for corona discharge due to the presence of different electric field profiles and space-charge effects in the discharge zone of the charger. The effect of high voltage waveform and frequency on the charging efficiency and penetration of nanoparticles should also be investigated.

In order to improve charging in real-time measurements of nanoparticles, the charger residence time should be investigated further. This may be done by improving the flow in the charger with a re-design and also by incorporating the distributed residence time into the charging model.

ACKNOWLEDGMENTS

This research was financially supported by the Thailand Research Fund (TRF), contract no. MRG5180217.

REFERENCES

Adachi, M., Kousaka, Y. and Okuyama, K. (1985). Unipolar and Bipolar Diffusion Charging of Ultrafine Aerosol Particles. *J. Aerosol Sci.* 16: 109–123.

Adachi, M., David, F.J. and Pui, D.Y.H. (1992). High-Efficiency Unipolar Aerosol Charger Using Radioactive Alpha Source. *J. Aerosol Sci.* 23: 123–137.

Alonso, M., Martin, M.I. and Alguacil, F.J. (2006). The Measurement of Charging Efficiencies and Losses of Aerosol Nanoparticles in a Corona Charger. *J. Electrostat.* 64: 203–214.

Alonso, M. and Alguacil, F.J. (2008). Particle Size Distribution Modification During and After Electrical Charging: Comparison between a Corona Ionizer and a Radioactive Neutralizer. *Aerosol Air Qual. Res.* 8: 366-380.

Biskos, G. (2004). *Theoretical and Experimental Investigation of the Differential Mobility Spectrometer*, Ph.D. Thesis, University of Cambridge, U.K.

Biskos, G., Mastorakos, E. and Collings, N. (2004). Monte-Carlo Simulation of Unipolar Diffusion Charging for Spherical and Non-Spherical Particles. *J. Aerosol Sci.* 35: 707–730.

Biskos, G., Reavell, K. and Collings, N. (2005a). Electrostatic Characterization of Corona-Wire Aerosol Charges. *J. Electrostat.* 63: 69–82.

Biskos, G., Reavell, K. and Collings, N. (2005b). Unipolar Diffusion Charging of Aerosol Particles in the Transition Regime. *J. Aerosol Sci.* 36: 247–265.

Biskos, G., Reavell, K. and Collings, N. (2005c). Description and Theoretical Analysis of a Differential Mobility Spectrometer. *Aerosol Sci. Technol.* 39: 527–541.

Boisdron, K. and Brock, J.R. (1970). On the Stochastic Nature of the Acquisition of Electrical Charge and Radioactivity by Aerosol Particles. *Atmos. Environ.* 4: 35–50.

Bricard, J. (1949). Ionic Balance of Lower Atmosphere. *J. Geophys. Res.* 54: 39–52. (in French)

Bricard, J. (1962). Fixation of Small Atmospheric Ions on Ultrafine Aerosols. *Geofisica Pura e Applicata.* 51: 237. (in French).

Brock, J.R. (1969). Aerosol Charging: the Role of Image Force. *J. Appl. Phys.* 41: 843–844.

Brock, J.R. (1970). Unipolar Diffusion Charging of Aerosols and the Image Force. *J. Colloid Interface Sci.* 33: 473–474.

Bucholski, A. and Niessner, R. (1991). Indirect Photoelectric Diffusion Charging of Submicron Aerosols. *J. Aerosol Sci.* 22: 111–115.

Burtscher, H., Scherrer, L. and Siegmann, H.C. (1982). Probing Aerosols by Photoelectric Charging. *J. Appl. Phys.* 53: 3787–3791.

Buscher, P., Schmidt-Ott, A. and Wiedensohler, A. (1980). Performance of a Unipolar "Square Wave" Diffusion Charger with Variable Nt-Product. *J. Aerosol Sci.* 25: 651–663.

Chen, D.R. and Pui, D.Y.H. (1999). A High Efficiency, High Throughput Unipolar Aerosol Charger for Nanoparticles. *J. Nanopart. Res.* 1: 115–126.

Cheng, S.H., Ranade, M.B. and Gentry, J.W. (1997). Experimental Design of High Volume Electrostatic Charger. *Aerosol Sci. Technol.* 26: 433–446.

Choi, Y. and Kim, S. (2007). An Improved Method for Charging Submicron and Nano Particles with Uniform Charging Performance. *Aerosol Sci. Technol.* 41: 259–265.

Ehrenhaft, F. (1925). The Electrical Behaviour of Radioactive Colloidal Particles of the Order of 10-5 cm as Observed Separately in a Gas. *Philos. Mag.* 49: 633–648.

Fuchs, N.A. (1947). On the Charging of Particles in Atmospheric Aerosols. *Izvestiia Akademii Nauk SSSR. Seriia Geograficheskaia i Geofizicheskaia.* 11: 341–348.

Fuchs, N.A. (1963). On the Stationary Charge Distribution on Aerosol Particles in a Bipolar Ionic Atmosphere. *Geofisica Pura e Applicata.* 56: 185–193.

Fuchs, N.A. and Sutugin, A.G. (1971). *High-Dispersed Aerosols.* Topics in Current Aerosol Research, Vol. 2, Pergamon Press, Elmsford, New York, U.S.A.

Gentry, J.W. and Brock, J.R. (1967). Unipolar Diffusion Charging of Small Aerosol Particles. *J. Chem. Phys.* 47: 64–69.

Graskow, B.R. (2001). *Design and Development of a Fast Aerosol Spectrometer*, Ph.D. Thesis, University of Cambridge, U.K.

Gunn, R. (1955). The Statistical Electrification of Aerosols by Ionic Diffusion. *J. Colloid Interface Sci.* 10: 107–119.

Han, B., Shimada, M., Choi, M. and Okuyama, K. (2003). Unipolar Charging of Nanosized Aerosol Particles Using Soft X-Ray Photoionization. *Aerosol Sci. Technol.* 37: 330–341.

Hewitt, G.W. (1957). The Charging of Small Particles for Electrostatic Precipitation. *AIEE Trans.* 76: 300–306.

Hernandez-Sierra, A., Alguacil, F.J. and Alonso, M. (2003). Unipolar Charging of Nanometer Aerosol Particle in a Corona Ionizer. *J. Aerosol Sci.* 34: 733–745.

Hinds, W.C. (1999). *Aerosol Technology*, John Wiley & Sons, New York, U.S.A.

Hontanon, E. and Kruis, F.E. (2008). Single Charging of Nanoparticles by UV Photoionization at High Flow Rates. *Aerosol Sci. Technol.* 42: 310–323.

Hutchins, D.K. and Holm, J. (1989). Aerosol Charger using Sinusoidally Driven Ion Current from a Corona Discharge. *Aerosol Sci. Technol.* 11: 244–253.

Intra, P. (2006). *Aerosol Size Measurement System Using Electrical Mobility Technique*, Ph.D. Thesis, Chiang Mai University, Thailand.

Intra, P. and Tippayawong, N. (2005) Approach to Characterization of a Diode Type Corona Charger for Aerosol Size Measurement. *KIEE Int. Trans. Electrophys. Appl.* 5–C: 196–203.

Intra, P. and Tippayawong, N. (2006a). Corona Ionizer for Unipolar Diffusion Charging of Nanometer Aerosol Particles. 29th Electrical Engineering Conference, Pattaya, Thailand, p. 1177–1180.

Intra, P. and Tippayawong, N. (2006b). Comparative Study on Electrical Discharge and Operation Characteristics of Needle and Wire-Cylinder Corona Chargers. *J. Electr. Eng. Technol.* 1: 520–527.

Intra, P. and Tippayawong, N. (2006c). An Electrical Mobility Spectrometer for Aerosol Size Distribution Measurement. Int. Conf. on Technology and Innovation for Sustainable Development, Khon Kaen, Thailand, p. 358–362.

Intra, P. and Tippayawong, N. (2006d). Aerosol Size Distribution Measurement Using Multi-Channel Electrical Mobility Sensor. *J. Aerosol Res.* 21: 329–340.

Intra, P. and Tippayawong, N. (2009a). Progress in Unipolar Corona Discharger Designs for Airborne Particle Charging: A Literature Review. *J. Electrostat.* 67: 605–615.

Intra, P. and Tippayawong, N. (2009b). Experimental Characterization of a Short Electrical Mobility Spectrometer for Aerosol Size Classification. *Korean J. Chem. Eng.* 26: 1770–1777.

Intra, P. and Tippayawong, N. (2010). Effect of Needle Cone Angle and Air Flow Rate on Electrostatic Discharge Characteristics of a Corona-Needle Ionizer. *J. Electrostat.* 68: 254–260.

Ivanov, V.D., Kirichenko, V.N. and Petryanov, I.V. (1969). Charging of Alpha-active Aerosols by Secondary Electron Emission. *Sov. Phys.* 13: 902–904.

Jaworek, A. and Krupa, A. (1989). Airborne Particle Charging by Unipolar Ions in AC Electric Field. *J. Electrostat.* 23: 361–370.

Jung, T., Burtscher, H. and Schmidt-Ott, A. (1988). Multiple Charging of Ultrafine Particles by Aerosol Phootemission (APE). *J. Aerosol Sci.* 19: 485–490.

Kascheev, V.A. and Poluektov, P.P. (1991). In. *Proceedings of European Aerosol Conference,* Influence of Laser Irradiation on Aerosol Particle Charging, Karlsruhe.

Keefe, D., Nolan, P.J. and Rich, T.Z. (1959). Charge Equilibrium in Aerosols According to the Boltzmann Law. *Proc. the R. Irish Acad.* 60: 27–45.

Kruis, F.E. and Fissan, H. (2001). Nanoparticle Charging in a Twin Hewitt Charger. *J. Nanopart. Res.* 3: 39–50.

Kulkarni, P., Namiki, N., Otani, Y. and Biswas, P. (2002). Charging of the Particles in Unipolar Coronas Irradiated by in-situ Soft X-ray: Enhancement of Capture Efficiency of Ultrafine Particles. *J. Aerosol Sci.* 33: 1279–1296.

Kulon, J. and Balachandran, W. (2001). The Measurement of Bipolar Charge on Aerosols. *J. Electrostat.* 51–52: 552–557.

Kulon, J., Hrabar, S. Machowski, W., and Balachandran, W. (2001). A Bipolar Charge Measurement System for Aerosol Characterization. *IEEE Trans. Ind. Appl.* 37: 472–479.

Kwon, S.B., Sakurai, H. and Seto, T. (2007). Unipolar Charging of Nanoparticles by the Surface-Discharge Microplasma Aerosol Charger (SMAC). *J. Nanopart. Res.* 9: 621–630.

Lawless, P.A. and Sparks, L.E. (1988). Modeling Particulate Charging in ESPs. *IEEE Trans. Ind. Appl.* 24: 922–925.

Lehtimaki, M. (1987). New Current Measuring Technique for Electrical Aerosol Analyzers. *J. Aerosol Sci.* 18: 401–407.

Liu, B.Y.H. and Pui, D.Y.H. (1975). On the Performance of the Electrical Aerosol Analyzer. *J. Aerosol Sci.* 6: 249–264.

Liu, B.Y.H., Whitby, K.T. and Yu, H.H.S. (1967a). On the Theory of Charging of Aerosol Particles by Unipolar Ions in the Absence of an Applied Electric Field. *J. Colloid Interface Sci.* 23: 367–378.

Liu, B.Y.H., Whitby, K.T. and Yu, H.H.S. (1967b). Diffusion Charging of Aerosol Particles at Low Pressures. *J. Appl. Phys.* 38: 1592–1597.

Marquard, A., Meyer, J. and Kasper, G. (2006). Characterization of Unipolar Electrical Aerosol Chargers—Part II: Application of Comparison Criteria to Various Types of Nanoaerosol Charging Devices. *J. Aerosol Sci.* 37: 1069–1080.

Matter, D., Mohr, M., Fendel, W., Schmidt-Ott, A., and Burtscher, H. (1995). Multiple Wavelength Aerosol Photoemission by Excimer Lamps. *J. Aerosol Sci.* 26: 1101–1115.

Medved, A., Dorman, F., Kaufman, S.L. and Pocher, A. (2000). A New Corona-Based Charger for Aerosol Particles. *J. Aerosol Sci.* 31: s616–s617.

Mirme, A. (1994). *Electric Aerosol Spectrometry*, Ph.D. Thesis, University of Tartuensis, Estonia.

Niessner, R., Schröder, H., Robers, W., and Kompa, K.L. (1988). Charging of Particles with Intense Visible Light Pulses. *J. Aerosol Sci.* 19: 491–500.

Park, D., An, M., and Hwang, J. (2007). Development and Performance Test of a Unipolar Diffusion Charger for Real-Time Measurements of Submicron Aerosol Particles Having a Log-Normal Size Distribution. *J. Aerosol Sci.* 38: 420–430.

Park, D., Kim, Y.H., Lee, S.G., Kim, C., Hwang, J. and Kim, Y.J. (2010). Development and Performance Test of a Micromachined Unipolar Charger for Measurements of Submicron Aerosol Particles having a Log-Normal Size Distribution. *J. Aerosol Sci.* 41: 490–500.

Park, K.T., Park, D., Lee, S.G. and Hwang, J. (2009). Design and Performance Test of a Multi-Channel Diffusion Charger for Real-Time Measurements of Submicron Aerosol Particles Having a Unimodal Log-Normal Size Distribution. *J. Aerosol Sci.* 40: 858 - 867.

Penney, G.W. and Lynch, R.D. (1957). Measurements of Charge Imparted to Fine Particles by a Corona Discharge. *AIEE Trans.* 76: 294–299.

Pui, D.Y.H. (1976) *Experimental Study of Diffusion Charging of Aerosols*, Ph.D. thesis, University of Minnesota, Minneapolis, U.S.A.

Pui, D.Y.H., Fruin, S. and McMurry, P.H. (1988). Unipolar Diffusion Charging of Ultrafine Aerosols. *Aerosol Sci. Technol.* 8: 173–187.

Qi, C., Chen, D.R. and Greenberg, P. (2008). Performance Study of a Unipolar Aerosol Mini-Charger for a Personal Nanoparticle Sizer. *J. Aerosol Sci.* 39: 450–459.

Reavell, K. (2002). Fast Response Classification of Fine Aerosols with a Differential Mobility Spectrometer. *Proceeding 13th Annual Conference Aerosol Society*, 121–124, Lancaster, U.K.

Schmidt-Ott, A., Schurtenbery, D. and Siegman, H.C. (1980). Enormous Yield of Photoelectrons for Small Particles. *Phys. Rev. Lett.* 45: 1284–1287.

Shimada, M., Okuyama, K., Inoue, Y., Adachi,M. and Fujii, T. (1999). Removal of Airborne Particles by a Device Using UV/Photoelectron Method under Reduced Pressure Conditions. *J. Aerosol Sci.* 30: 341–353.

Tammet, H., Mirme, A. and Tamm, E. (1998). Electrical Aerosol Spectrometer of Tartu University. *J. Aerosol Sci.* 29: s427–s428.

Tammet, H., Mirme, A. and Tamm, E. (2002). Electrical Aerosol Spectrometer of Tartu university. *Atmos. Res.* 62: 315–324.

Tsai, C.J., Chen, S.C., Chen, H.L., Chein, H.M., Wu, C.H. and Chen, T.M. (2008). Study of a Nanoparticle Charger Containing Multiple Discharging Wires in a Tube. *Separation Sci. Technol.* 43: 3476–3493.

Tsai, C.J., Lin, G.Y., Chen, H.L., Huang, C.H. and Alonso, M. (2010). Enhancement of Extrinsic Charging Efficiency of a Nanoparticle Charger with Multiple Discharging Wires. *Aerosol Sci. Technol.* 44: 807–816.

TSI Incorporated. (2004a). *Operation and Service Manual*, Revision B, for Engine Exhaust Particle SizerTM Spectrometer, Model 3090, Minnesota, U.S.A.

TSI Incorporated. (2004b). *Operation and Service Manual*, Revision B, for Electrical Aerosol DetectorTM Spectrometer, Model 3070, Minnesota, U.S.A.

Unger, L., Ehouarn, P. and Borra, J.P. (2000). Influence of Aerosol Deposition on the Charging Efficiency of a Corona Charger. *J. Aerosol Sci.* 31: s612–s613.

Unger, L., Boulaud, D. and Borra, J.P. (2004). Unipolar Field Charging of Particles by Electric Discharge: Effect of Particle Shape. *J. Aerosol Sci.* 35: 965–979.

Whitby, K.T. (1961). Generator for Producing High Concentration of Small Ions. *Rev. Sci. Instrum.* 32: 1351–1355.

Whitby, K.Y. and Clark, W.E. (1966). Electric Aerosol Particle Counting and Size Distribution Measuring System for the 0.015 to 1 μm Size Range. *Tellus.* 18: 573–586.

White, H.J. (1951). Particle Charging in Electrostatic Precipitation. *AIEE Trans.* 70: 1186–1191.

White, H.J. (1963). *Industrial Electrostatic Precipitation*, Addison-Wesley, Reading, U.S.A.

Wiedensohler, A. (1988). An Approximation of the Bipolar Charge Distribution for Particles in the Submicron Size Range. *J. Aerosol Sci.* 19: 387–389.

Wiedensohler, A., Buscher, P., Hansson, H.C., Martinsson, B.G., Stratmann, F., Ferron, G. and Busch, B. (1994). A Novel Unipolar Charger for Ultrafine Aerosol Particles with Minimal Particle Losses. *J. Aerosol Sci.* 25: 639–649.

Willeke, K. and Baron, P.A. (1993). *Aerosol Measurement: Principles, Techniques, and Applications*, John Wiley & Sons, New York, U.S.A.

Yeh, H.C. (1976b). A Theoretical Study of Electrical Discharging of Self-charging Aerosols. *J. Aerosol Sci.* 7: 343.

Yeh, H.C., Newton, G.J., Raabe, O.G. and Boor, D.R. (1976). Self-charging of 198Au Labelled Monodisperse Gold Aerosols Studied with a Minature Electrical Mobility Spectrometer. *J. Aerosol Sci.* 7: 245–253.

Received for review, October 2, 2010
Accepted, February 23, 2011